De la Cueva-Alique, I. et al. (2019) 'Water soluble, optically active monofunctional Pd() and Pt() compounds: promising adhesive and antimigratory effects on human prostate PC-3 cancer cells', Dalton transactions : an international journal of inorganic chemistry, 48(38), pp. 14279–14293.

Available at https://doi.org/10.1039/C9DT02873K

Dalton Transactions

ARTICLE

Water soluble, optically active monofunctional Pd(II) and Pt(II) compounds: Promising adhesive and antimigratory effects on human prostate PC-3 cancer cells.

Received 00th January 20xx,
Accepted 00th January 20xx

DOI: 10.1039/x0xx00000x

www.rsc.org/

Isabel de la Cueva-Alique,[a] Laura Muñoz-Moreno,[b] Elena de la Torre-Rubio,[a] Ana M. Bajo,[b] Lourdes Gude,[a] Tomás Cuenca,[a] Eva Royo*[a]

New water soluble, enantiopure palladium and platinum compounds R_N-[M{(1*S*,4*R*)-κNOH,κ^{2}NH(2-pic)}Cl]Cl and S_N-[M{(1*R*,4*S*)-κNOH,κ^{2}NH(2-pic)}Cl]Cl (2-pic = 2-picolyl, M = Pd **1** and **1'**, Pt **2** and **2'**, respectively), and heterometallic Pd/Ti [(η^5-C_5H_5)$_2$Ti{(1S,4R)-κON,κ^{2}NH(2-pic)}(PdCl)]Cl (**3**) have been synthesized. The novel compounds were fully characterized by NMR spectroscopy and CHN elemental analysis and **1**, **1'**, **2** and **2'** were further evaluated by polarimetry, ultra-violet and circular dichroism spectroscopy. Aqueous stability of novel compounds was studied by NMR spectroscopy under physiological conditions and the new species detected under such conditions have been characterized by NMR techniques and HR-ESI-MS (High-Resolution Electrospray Ionization Mass Spectrometry). Compound-DNA interactions have been investigated for the palladium and platinum compounds by equilibrium dialysis, Fluorescence Resonance Energy Transfer (FRET) DNA melting assays and viscometric titrations, revealing a better binding affinity and ability to affect duplex DNA of the palladium compounds. Metal derivatives have been tested *in vitro* against three cancer (prostate PC-3, cervical HeLa and breast MCF-7) and one non-tumorigenic (human prostate RWPE-1) cell lines. Highest anticancer activities were shown by palladium compounds **1**, **1'** in all cancer lines, although their toxicity was lower to that found for cisplatin. Most importantly, the effect of the compounds on cell adhesion and migration of the androgen-independent prostate cancer PC-3 cells has been assessed, and the efficacy of Pd enantiomers to affect the invasive phenotype of PC-3 cells has been demonstrated.

Introduction

Despite the widespread use in clinic of cisplatin (cis-diamminedichloroplatinum(II)) and second-generation platinum compounds as anticancer drugs,[1] their accompanying disadvantages (i.e., active in a limited spectrum of tumours, systemic toxicity, the induction of resistance and the lack of selectivity) have prompted many scientists being involved in the design of metal compounds with non-classical anticancer mechanisms of action.[2–10] Since binding of cisplatin to DNA is generally accepted to be responsible for the cytotoxicity of this drug,[10–12] the design of innovative platinum structures, which affect DNA (or other biological targets, as proteins or enzymes) differently, could afford new anticancer agents with a different spectrum of biological activity, accompanied by a better toxicological and pharmacokinetics profile.[3,4,12–14] Within this context, the so-called monofunctional compounds have emerged as a promising type of modern platinum anticancer agents. Among them, compounds with non-intercalating potential, tricoordinated N-based chelating ligands have scarcely been explored.[12,14–18]

Among all the metal ions investigated, there is considerable interest in studying Pd(II) complexes as anticancer drugs,[19–23] due to the many similarities between Pt(II) and Pd(II). However, the aquation and ligand-exchange rates of Pd(II) complexes are about 10^5 times faster than those of the Pt(II) analogues,[24] which is considered an important handicap of palladium-based drugs. The hypothesis is that the higher reactivity could prevent the palladium compounds to reach their target (DNA) by favouring interactions with other donor species present in the bloodstream, increasing their toxicity and lowering their therapeutic potential. Thus, in order to make palladium complexes competitive anticancer agents, a proper choice of ligands seems to be crucial.[19–23] Recent studies demonstrate that several Pd(II) compounds showed a highly efficient biological activity *in vitro*, often significantly better than their Pt(II) counterparts or cisplatin.[21,25] In addition, the palladium compounds have, in general, better solubility compared to Pt(II) analogues.[20,22]

On the other hand, the effect of stereochemistry on biological activity is of great importance in medicinal chemistry.[26,27] Anticancer properties of chiral platinum derivatives have been largely studied,[28–36] but the role of the stereochemistry in the biological activity of palladium-based compounds has been comparatively less investigated.[37–46] With the aim in mind of preparing optically active palladium and platinum compounds,

[a] Departamento de Química Orgánica y Química Inorgánica, Instituto de Investigación en Química Andrés del Río (IQAR), Universidad de Alcalá, 28805 Alcalá de Henares, Madrid, Spain.
[b] Departamento de Biología de Sistemas, Facultad de Medicina y Ciencias de la Salud, Universidad de Alcalá, 28805 Alcalá de Henares, Madrid, Spain.

†Electronic Supplementary Information (ESI) available: Representative NMR, UV-vis, CD spectra and FRET-melting curves of compounds **1**, **1'**, **2**, **2'** and **3.** See DOI: 10.1039/x0xx00000x

natural terpenes are useful building blocks, since they are enantiomerically pure, commercially available low-cost reagents which can be tailored by known stereoselective functionalization procedures.[47,48] In the last years, we have used chiral amino-oxime organic compounds derived from *R*- and *S*-limonene to prepare water soluble, enantiopure Ru(II) and Ti(IV) compounds with relevant antitumor properties.[49–52] The p-cymene ruthenium(II) amino-oxime containing compound has shown an inhibition of tumour growth by 45 % in a preliminary *in vivo* assay of PC-3 xenografts in nude mice.[49] Amino and specially oxime functional groups possess hydrogen-bonding capabilities,[53–55] and they are excellent chemical frameworks for the design of soluble and stable in biological media metal compounds. The use of oxime-containing ligands have additional advantages, since organic derivatives with oxime groups have been reported to exert some interesting biological properties (i.e., inhibit several protein kinases[56–58] and have shown anti-inflammatory, analgesic, bactericidal, antiviral and anticancer activities). In addition, examples of anticancer oxime containing Pt,[59,60] Pd,[61,62] Rh, Ir,[63] and Ru[64,65] derivatives have been reported as non-classical anticancer agents with interesting anti-tumour properties and different DNA interactions to that of cisplatin.

As a part of an ongoing research project, we were interested in how the use of the potentially tridentate, enantiopure (2-pic)amino-oxime pro-ligands derived from *R*- or *S*-limonene (Fig.1) could benefit the biological anticancer profiles of Pd(II) and Pt(II) compounds.

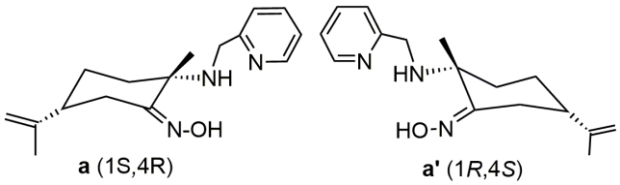

a (1S,4R) **a'** (1*R*,4*S*)

Fig.1. Optically active (2-pic)amino-oxime pro-ligands used in this report.

We report herein the synthesis and characterization of two pairs of palladium and platinum enantiomers containing a N-based tridentate (2-pic)amino-oxime ligand. The amino-oximato heteronuclear Ti(IV)/Pd(II) compound is reported as well. Lipophilicity of the novel metal compounds was evaluated by means of the n-octanol/water partition coefficients and their behaviour in physiological relevant conditions was studied by ^{1}H-NMR spectroscopy. In addition, we describe some important biological properties of the compounds (i.e, their DNA interactions, their cytotoxic behaviour against three cancer and one non-tumorigenic cell lines, and their effects on the adhesion and migration abilities of PC-3 cells).

Results and discussion

Synthesis and characterization of metal compounds

The reactions of $K_2[MCl_4]$ (M = Pd, Pt) with enantiomerically pure amino-oxime derivatives (1*S*,4*R*)- or (1*R*,4*S*)-{NOH, NH(2-pic)} (2-pic = 2-picolylamine **a**, **a'**) afford new amino-oxime palladium and platinum cationic compounds R_N-[M{(1*S*,4*R*)-κNOH,κ^{2}NH(2-pic)}Cl]Cl or S_N-[M{(1*R*,4*S*)-κNOH,κ^{2}NH(2-pic)}Cl]Cl, respectively (M = Pd **1**, **1'**; M = Pt **2**, **2'**) (Fig. 2).

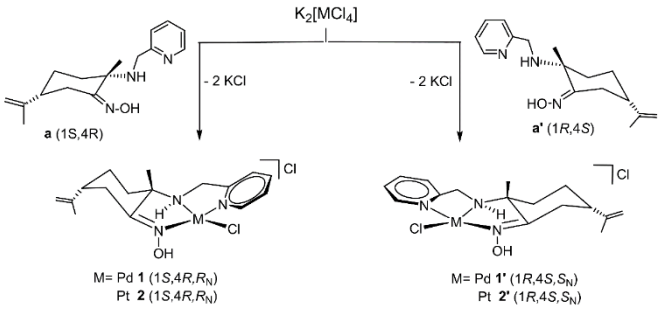

Fig. 2. Synthesis of novel enantiomerically pure palladium and platinum compounds.

Since Pd(II) and Pt(II) compounds have a new stereogenic centre at the amino ligand, two different diastereomers, (1*S*,4*R*,S_N), (1*S*,4*R*,R_N)-**1**, -**2** and (1*R*,4*S*,S_N), (1*R*,4*S*,R_N)-**1'**, -**2'**, distinguishable by NMR spectroscopy, could be formed. ^{1}H, ^{13}C and ^{15}N NMR spectra in chloroform-d_1 of the solids obtained show the existence of only one diastereomer in solution, namely (1*S*,4*R*,R_N)-**1**, -**2** and (1*R*,4*S*,S_N)-**1'**, -**2'**.

As expected for enantiomer pairs, analytical and spectroscopic data of **1** and **2** are identical to those observed for **1'** and **2'**, respectively (see Experimental Section and Fig. S3, S4, S9, S10, ESI). Calculated data of specific optical rotation in chloroform solution for the pro-ligands and novel metal derivatives ($[\alpha]^{23}_D$ (deg·dm^{-1}·dL·g^{-1}) = +127 ± 1.3 **a**, -126 ± 1.3 **a'**, -23.1 ± 1.8 **1**, +23.8 ± 1.8 **1'**, -32.9 ± 1.8 **2**, +33.1 ± 1.8 **2'**) also evidence the enantiomeric relationship of the stereoisomers.

The UV-vis spectrum of **1** or **1'** in water (Fig. S14, ESI) shows an intense absorption band at 267 nm, and an additional, broad band at 334, while **2** or **2'** spectrum (Fig. S15, ESI) shows one intense absorption band at 274 nm. Enantiomers **1**, **1'** and **2**, **2'** were also investigated by Circular Dichroism (CD) spectroscopy in water. The pair of palladium enantiomers give complementary CD spectra (Fig. S16, ESI), with opposite Cotton effects at 226, 243, 266, 300, 328 and 400 nm. The derivatives of platinum (**2** and **2'**) show opposite Cotton effects at 221, 248, 273, 321 and 369 nm. Although CD cannot give information on the absolute configuration of the compounds, the results confirm that the molecular structures of **1** and **1'** or **2** and **2'** are mirror images.[66]

Full NMR spectroscopy characterization of the new compounds, achieved with the help of bidimensional ^{1}H–^{1}H COSY, ^{1}H–^{13}C HSQC, HMBC and ^{1}H-^{15}N HMBC experiments, is consistent with the (2-pic)amino-oxime acting as a tridentate ligand. The changes in the ^{1}H NMR spectra of the complexes compared to those of free pro-ligands **a** and **a'** are most dramatic for the signals of protons in close vicinity to coordinated N atoms. Thus, ^{1}H NMR spectra of **1**, **1'** and **2**, **2'** show broad resonances at δ 10.61 and 10.51, respectively, assigned to NH protons and downfield shifted relative to NH protons of metal free amino-oxime derivatives (δ 2.60 **a**, **a'**). NOH resonances (assigned with the help of ^{1}H–^{13}C HSQC, HMBC experiments, see Fig. S6, ESI)

shift from δ 9.80 (**a**, **a'**) to δ 8.95 **1**, **1'** and 9.23 **2**, **2'**, while methylene protons –C*H*$_2$-C_5H_4N move downfield (δ 4.53, 4.45 **1**, **1'**; δ 4.63, 4.43 **2**, **2'**) relative to the resonances observed in pro-ligands **a**, **a'** (δ 3.87, 3.61). Similar behaviour is observed for the resonances of C*q*=NOH (175.9 **1**, **1'**; 175.4 **2**, **2'**), ***C*$_{ipso}$**(NC_5H_4) (165.7 **1**, **1'**; 167.5 **2**, **2'**), C*q*NH (69.6 **1**, **1'**; 70.6 **2**, **2'**) and –***C***H_2(NC_5H_4) (51.9 **1**, **1'**; 52.0 **2**, **2'**), which shift downfield relative to the signals detected in ^{13}C NMR spectra of **a**, **a'** (162.4, 161.1, 56.9, 48.1).

The difference between the chemical shifts of the nitrogen signals arising from the oxime, pyridine and amino groups in **a**, **a'** (δ 346.7 *N*OH, δ 305.3 C_5H_4*N* and δ 51.8 NH) and those found in compounds **1**, **1'** (δ 258.2 *N*OH, δ 220.7 C_5H_4*N* and δ 61.2 NH) and **2**, **2'** (δ 245.0 *N*OH, δ 208.2 C_5H_4*N* and δ 48.8 NH) ratifies the proposed tridentate coordination of the ligand for these Pd(II) and Pt(II) compounds.

To confirm the cationic character and the tricoordination of the ligand, we carried out the reaction of **1**, **2** with KPF_6. The reactions in dichloromethane proceed in 24 h at room temperature to afford yellow solids, whose ^{19}F and ^{31}P NMR spectra in dichloromethane-d_2 show the presence of the counteranion $[PF_6]^-$. The similar chemical shifts of the nitrogen resonances found in ^{1}H-^{15}N HMBC NMR spectra of **1**, **2** and **1·PF$_6$**, **2·PF$_6$**, respectively, also validate the coordination of the (2-pic)amino-oxime ligand through all three N-donors.[17,67,68]

Despite the efforts made, single, quality crystals of the compounds could not be obtained. However, absolute configuration of the amino nitrogen is endorsed by bidimensional NOESY experiments. NOESY spectra revealed the association of the NH amino proton with the resonance due to one hydrogen of the CH_2[6] fragments (δ 2.80 **1**, **1'** and δ 2.82 **2**, **2'**) (see Fig. 3. and Fig. S8, S13, ESI).

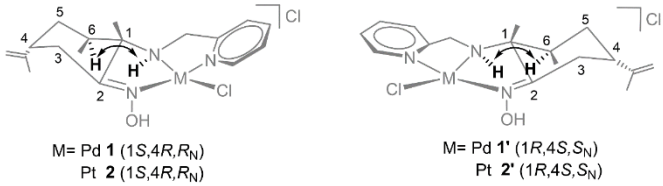

Fig. 3. Associated proton resonances detected in the bidimensional NOESY spectra of compounds **1**, **2** and **1'**, **2'**.

Epimerization was not observed in chloroform-d_1 or methanol-d_4 solutions over time, within a temperature range of 10-40 °C, suggesting a preferred coordination mode of the N,N,N tridentate ligand. Stereoselective coordination of optically active chelating ligands derived from natural terpenes have been previously reported.[49,69–72]

IR spectra of (2-pic)amino-oxime pro-ligands **a**, **a'** exhibit strong, broad ν(OH/NH) bands at ῡ 3086–3314 cm^{-1} and C=N stretching frequencies at ῡ 1643, 1595 cm^{-1}.[52] IR spectra of palladium and platinum novel compounds show sharp absorptions at ῡ 3324 and 1642, 1613 (**1**, **1'**), and 3336 and 1642, 1610 (**2**, **2'**) cm^{-1}, assigned to ν(OH/NH) bands and C=N stretching frequencies.

A variety of heterometallic complexes have been evaluated as anticancer agents with the assumption that combination of different cytotoxic metals in the same molecule can result in enhanced anti-tumour efficacy.[73,74,83–85,75–82] Within this frame, examples of heterometallic palladium complexes tested as anticancer agents are scarce.[75,79,86,87] On this basis, we decided to incorporate a palladium centre into our previously described titanium compound [(η^5-C_5H_5)$_2$Ti{(1*S,4R*)-κON,NH(2-pic)}Cl] ((1*S,4R*)-**Ti**),[50,51] which displays some of the lower IC_{50} values described so far in PC-3 and Caki-1 cancer cell lines for mononuclear titanocene derivatives.

Treatment of (1S,4R)-**Ti** with [Pd(COD)Cl$_2$] allows isolation of novel heterometallic titanium/palladium complex [(η^5-C_5H_5)$_2$Ti{(1S,4R)-ON,NH(2-pic)}(PdCl)]Cl (**3**). The same compound was also obtained from the reaction of [(η^5-C_5H_5)$_2$TiCl$_2$] (TDC), the palladium compound **1** and NEt_3 (Fig. 4).

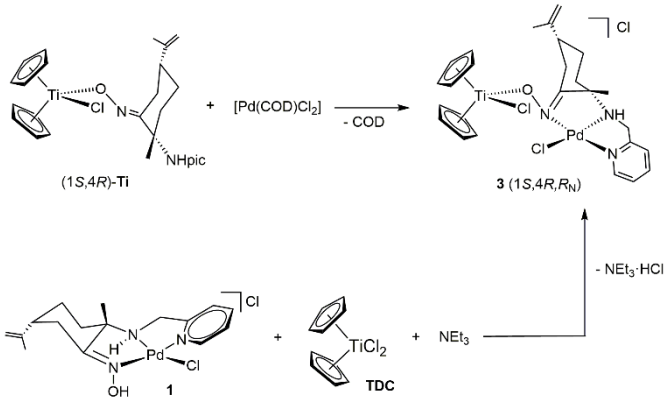

Fig. 4. Synthesis of novel Ti/Pd heterometallic derivative **3**.

The reaction of **3** with KPF_6 in dichloromethane affords an orange solid, whose ^{19}F and ^{31}P NMR spectra in dichloromethane-d_2 confirm the presence of the counteranion $[PF_6]^-$ (See Experimental Part).

Again, amino coordination to the palladium centre can give rise to different stereoisomers of absolute configuration (1*S*,4*R*,*S*$_N$)-**3**, (1*S*,4*R*,*R*$_N$)-**3**. ^{1}H, ^{13}C and ^{15}N NMR spectra of **3** show the existence of only one diastereomer in solution. The 2D NOESY spectrum of **3** revealed the interaction between NH (δ 10.89) and CH_2[6] protons (δ 2.82), and support the (1*S*,4*R*,*S*$_N$) absolute configuration proposed for compound **3** (Fig. S20, ESI).

^{1}H NMR spectra of **3** show a broad resonance at δ 10.89 assigned to NH hydrogen atom while the downfield =NOH proton signal observed in the spectra of free ligand **a** or palladium compound **1** disappears after reaction with the metallocene, which proves oxime deprotonation in the final heterometallic complex. The proposed tricoordination of the (2-pic)amino-oximato ligand to palladium is validated by ^{13}C and ^{15}N-^{1}H HMBC NMR data. Thus, chemical shift of the ^{13}C NMR resonance due to *Cq*=NO (δ 176.2 **3**) is similar to that assigned to *Cq*=NOH in compound **1** (δ 175.9) and differs in 18.3 ppm from the resonance due to the quaternary oximato carbon found in (1*S,4R*)-**Ti** (δ 157.6). The ^{13}C NMR resonances assigned to ***C***H_2(NC_5H_4) (δ 51.4 **3**) and *Cq*NH (δ 67.2 **3**) are also similar to those observed in compound **1** (δ 51.9 and 69.6, respectively). Comparison of ^{15}N-^{1}H HMBC NMR spectra of compound **3** (δ

301.4 =*N*O, δ 220.9 *N*C_5H_4 and δ 60.7 NH) with those of metallocene (1*S*,4*R*)-**Ti** (δ 402.1 =*N*O, δ 312.15 *N*C_5H_4 and δ 52.6 NH) and **1** (δ 258.2 =*N*OH, δ 220.7 *N*C_5H_4 and δ 61.2 NH) also validates the proposed structure for this heterometallic compound.

Behaviour of metal compounds 1, 2 and 3 under physiological conditions.

Phosphate buffered (PB) or phosphate buffered saline (PBS) solutions were used in the *in vitro* biological and DNA-metal compounds interactions assays. With this in mind, the behaviour of the novel palladium and platinum metal compounds was evaluated by pH and time dependent ^{1}H NMR in water-d_2 and solutions of PB or PBS in deuterated water.

Upon dissolution in water-d_2, ^{1}H NMR spectra of **1** or **2** show a single set of resonances, which suffer no apparent changes in the following 72 h within the 0-3.0 pH interval and in the absence or presence of NaCl ([NaCl] = 0-200 mM (Fig. S21, S32, ESI). ^{1}H-^{15}N HMBC NMR spectra of **1**, **2** in water-d_2 showed nitrogen resonances analogous to those found in the chloroform-d_1 spectra. After evaporation of water, ^{1}H NMR resonances in chloroform-d_1 of the samples coincide with those obtained for **1**, **2**, and their HR-ESI-MS show molecular peaks with the correct isotopic pattern for $[M\text{-}Cl]^+$ at m/z = 416.0542 (100 %) **1** and 504.1149 (100%) **2**. These experimental data evidence the stability of novel compounds **1** and **2** in such conditions, plausibly favoured by strong intramolecular hydrogen bond M-Cl···H-O=N contacts. Such short intramolecular interactions have been confirmed by X-ray studies of a variety of oxime containing palladium and platinum compounds.[70,88–90]

When deuterated PB, PBS or basified water-d_2 (pH* = 7.4 where pH* = pHmeter reading in water-d_2) solutions of **1** were monitored by ^{1}H NMR spectroscopy (Fig. S22, ESI), a different, new set of signals was detected, which remained the same for the next 72-120 h at room temperature within the 4.0-11 pH range. HR-ESI-MS of the samples afforded a molecular peak with the correct isotopic pattern for $[2M\text{-}2Cl\text{-}2H]^{2+}$ at m/z = 379.0784 (100 %). Thus, this new species was tentatively assigned to a doubly bridged k^{2}NO oximato dinuclear palladium compound.

In contrast, ^{1}H NMR time dependent spectra of **2** in buffered or basified solutions showed, 1 h after dilution, a mixture of resonances, assigned to compound **2** and at least two new different derivatives. After 60-72 h, the mixture resolved into a single set of resonances, which remained stable for the next 48 h under the same temperature and pH conditions (within the 6-10 pH interval) (Fig. S33, ESI). Again, HR-ESI-MS of the samples showed a molecular peak with the correct isotopic pattern for $[2M\text{-}2Cl\text{-}2H]^{2+}$ at m/z = 467.1387 (100 %), which confirms a similar dehydrochlorination process for the Pt(II) compound.

Acidification of such deuterated basified solutions with DCl to final pH* = 0-2 yields reversible, quantitative formation of compounds **1** or **2**, respectively.

The species present at physiological pH have been fully characterized by NMR. ^{15}N NMR HMBC spectra validates deprotonation of the –NOH oxime group. Thus, resonances ascribed to the k^{2}NO nitrogen atoms are low field shifted (values at pH = 7.4: δ 296.3 **1**, 274.4 **2**) relative to the N oxime signal observed for compound **1** or **2** in water-d_2 at acidic pH values. In addition, 2D NOESY spectrum revealed the association of one of the aromatic pyridyl protons with the resonance assigned to one hydrogen of the CH_2[3] fragment (δ 3.51 **1**, 3.45 **2**) (Fig. S31, S41, ESI and numbered pro-ligand in Fig. 3). Such NOESY contacts implies dinuclear structures for both deprotonated species.

An analogous process has been reported by Watanabe et al in a cyclopentadienyl chlorido oxime Ir(III) compound, which undergoes dehydroclorination with equimolar amounts of base to afford a doubly bridged oximato dinuclear species.[91]

It is important to note that such dinuclear species contain one labile, O-based position at each metal center, whose substitution by softer Lewis base donors would cleave the Pd-O bond to render kNO oximato monometallic compounds.

The stability of heterometallic **3** in water was studied as well, by monitoring water-d_2 solutions of the compound (15 mM, pH* = 3.8) by ^{1}H NMR. The first spectrum taken following water-d_2 addition revealed the complete hydrolysis of **3**. Accordingly, the spectrum shows a singlet at δ 6.60 ascribed to titanium bound cyclopentadienyl species, which has been previously assigned to $[Cp_2Ti(OH)(H_2O)]^{+}$[50,92,93] (Fig. S42, ESI). Besides this resonance, the set of signals assigned to palladium compound **1** in water-d_2 were detected. Under physiological conditions (pH* = 7.4), resonances due to cyclopentadiene are detected together with deprotonated dinuclear palladium derivative in the ^{1}H NMR spectrum.

Lipophilicity

Lipophilicity/hydrophobicity is one of the most important physicochemical properties related to the pharmacokinetic behavior of drug-like molecules.[94–99] The partition coefficient between water and *n*-octanol (log*P*) have been used to predict the permeability of drugs, since there is good correlations between intestinal permeability and physicochemical parameters such as lipophilicity.[97] We determined the *n*-octanol/water partition coefficient of derivatives **1** and **2** by using the shake-flask method[96,100] at room temperature. The estimated values (log*P*o/w = -1.99 ± 0.3 **1** and –0.42 ± 0.06 **2**) indicate that **1** is more hydrophilic than **2**. This result is consistent with the water solubility of the compounds, which follows the order **1** >> **2** (ca. 84.3 and 13.3 mM in water, respectively). The palladium complex has a partition coefficient close to that reported for cisplatin (log P = -2.27),[98,99] while the platinum analogue turned out to be more lipophilic than the clinical metalodrug. The lack of stability in water of heterometallic compound **3** precluded measurement of its partition coefficient.

DNA-metal compound interaction studies

Traditionally, DNA has been considered one of the main cellular targets of platinum- and palladium-based drugs. Structurally, the novel compounds **1**, **1'**, **2** or **2'** as well as the species detected under physiological pH* values, belong to the so called

"rule breakers",[14,15,101,102] as they do not adjust to the conventional anticancer platinum compounds. Thus, we were interested in exploring the structure-DNA interactions relationships of these monofunctional Pd and Pt derivatives. Again, the lack of stability in water of compound **3** made unfeasible a similar study for the Ti/Pd derivative.

The interactions with double-stranded (ds) DNA were assessed by equilibrium dialysis, fluorescence-based DNA melting experiments and DNA viscosity titrations.

Dialysis experiments with Calf Thymus (CT) DNA were carried out first to establish whether the metal complexes were able to bind ds DNA and to determine apparent binding constants. In these experiments, metal complex solutions were incubated with CT DNA at room temperature for 24 hours, after which the amount of compound bound to DNA was quantitated. Experiments were run based on adaptation of the protocol described by Chaires,[103] with the modifications described in the Experimental section. The results obtained for compounds **1**, **1'**, **2** and **2'** are summarized in Table 1.

Table 1. DNA apparent association constants of compounds **1**, **1'**, **2**, **2'** obtained by equilibrium dialysis.[a]

Compound	1	1'	2	2'
K_{app} (M^{-1}) x 10^{-5}	1.14 ± 0.07	1.00 ± 0.20	0.14 ± 0.01	0.23 ± 0.02

[a] Apparent association constants were calculated according to the equation $K_{app} = C_b/(C_f)(S_{total}-C_b)$, where C_b is the amount of metal complex bound, C_f is the free metal complex concentration and S_{total} = 75 μM, in monomeric units (bp).

Table 1 shows that the metal complexes bind ds DNA with good affinity, especially in the case of palladium compounds **1** and **1'**, which displayed apparent association constants in the order of 10^5 M^{-1}. Despite the fact that no significant differences in DNA affinity were found between **1** and **1'**, platinum compounds **2** and **2'** did exhibit some differential binding affinity, with the (1*R*,4*S*,S_N)-enantiomer having almost a two-fold larger binding constant than the (1*S*,4*R*,R_N)-isomer. Overall, palladium metal complexes presented values of apparent binding constants between 5- and almost 10-fold higher than their platinum counterparts.

We were also interested in determining the effect that the binding of these compounds may exert on DNA denaturing temperature (Tm), as the ligand portion of these metal complexes contains an aromatic ring that could intercalate between DNA base pairs. For that purpose, we used a *variable-temperature (FRET-melting) assay*, an experiment that reduces DNA consumption allowing the testing of a wide range of compound concentrations. The assay has been extensively used in the last years to determine the degree of thermal stabilization of different DNA structures in the presence of potential binders.[104] Thus, fluorescence resonance energy transfer (FRET) experiments were used to establish whether either the precursor ligands **a** and **a'** or the metal complexes **1**, **1'**, **2** and **2'** were able to thermally stabilize ds DNA structures.

A 10-bp oligonucleotide designated as F10T, labelled with two fluorophores, FAM at its 5' end and TAMRA at the 3' end, was used in these experiments.[105] If the metal complex binds to DNA affecting the stability of the double helix, changes in the value of DNA Tm should be observed. Stabilization of duplex DNA via an intercalation mechanism usually results in increased values of Tm.

The different compounds were analysed using a wide range of concentrations, from 1 μM to an excess of 10 μM. Under these conditions, the complexes did not produce a significant change in the DNA melting temperature in the lower concentration range (Representative example in Fig. S43, ESI). Overall, these results seem to suggest that the compounds may interact with DNA through recognition of the DNA grooves and/or by an external electrostatic fashion.

On the other hand, at high concentrations, compounds **1** and **1'** were able to slightly destabilize the duplex structure (ΔTm= -3 °C at 10 μM, Fig. S43, ESI). Furthermore, a more significant effect was observed in the reverse folding process, in which a concentration of metal complex above 2-3 μM produced a significant distortion in the thermal curve, suggesting that high concentrations of the compounds prevented proper annealing of the two DNA strand to regenerate the duplex structure. On the other hand, neither the precursor ligands **a** or **a'**, nor the metal complexes **2** and **2'** showed any significant analogous effect on DNA melting or folding profiles along the 1-10 μM concentration range.

Finally, *DNA viscosity titrations* were performed as they provide a simple and fast way to discriminate between the different binding modes of DNA ligands (especially non-covalent, such as intercalation *versus* groove or external binding).[106] From gradual DNA titration with the compounds of interest, linear plots of the cubic root of the relative DNA viscosity $(\eta/\eta_o)^{1/3}$ versus the molar ratio of bound ligand to DNA nucleotide (r) can be obtained.[107] The slope values are used to determine the DNA-ligand binding modes. Groove binding compounds usually display a slope close to 0.0 (experimentally in the range -0.3 to 0.2), whereas classical mono-intercalants result in a slope close to 1.0.[106–108]

All metal complexes, **1**, **1'**, **2** and **2'**, showed a linear $(\eta/\eta_o)^{1/3}$ versus r correlation with the compound to DNA ratio used in the experiments and produced a slight decrease of DNA viscosity at increasing concentrations, with negative slope values of -0.26, -0.23, -0.14 and -0.14, respectively (Fig. 5). This decrease is significantly lower than the effect that a compound such as cisplatin, known to covalently bind to DNA through metalation of the N7 of purines, exerts when it binds to the DNA double helix.

The results from the viscosity experiments revealed that the metal complexes do not interact with double stranded DNA by inserting the pyridine ring of the ligand between the base pairs, thus a classical intercalating interaction can be discarded. This was already expected, considering the relatively small surface of the pyridine ring. Although the viscosity slope values fell within the experimental values obtained for typical groove binding ligands, the negative slope are suggestive of a slight shortening of the DNA double helix, giving rise to an overall effect of DNA compaction. It has been previously reported that some metal complexes can bind DNA by a partial or non-

classical intercalation which results in a decrease of the DNA contour length by bending or kinking the DNA helix.[109–111]
On the other hand, platinum(II) compounds with only one labile ligand are known to produce monofunctional adducts with DNA, which causes less distortion in the overall structure of the DNA double helix than cisplatin.[12,112–114]
Overall, the different experiments confirmed DNA recognition by the metal complexes reported herein, especially in the case of palladium compounds, which have shown a higher binding affinity and more significant effects on ds DNA thermal and hydrodynamic properties.

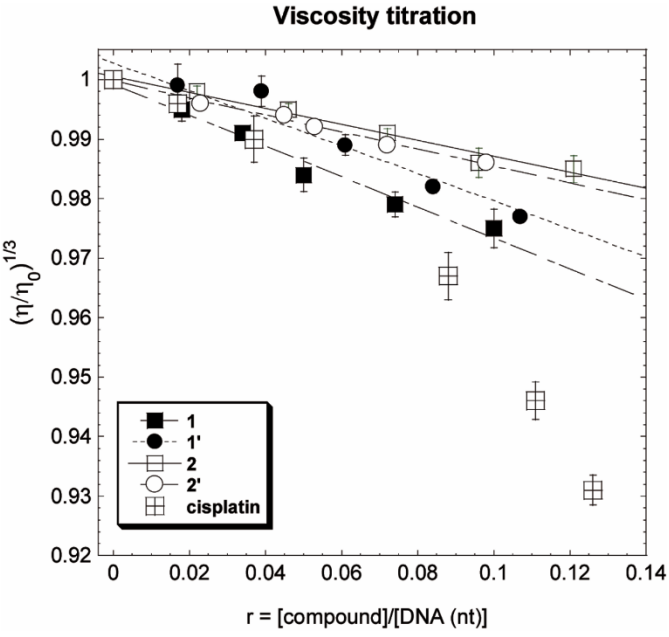

Fig. 5. Viscometric titrations of *Calf Thymus* (CT) DNA and metal complexes **1**, **1'**, **2** and **2'**, at 25 °C (10 mM sodium phosphate buffer, pH 7.2). Cisplatin is included for comparison.

***In vitro* cell studies**

The cytotoxic activity of pro-ligands **a·HCl**, **a'·HCl**, titanocene (1*S*,4*R*)-**Ti**, cisplatin, and novel metal compounds **1**, **1'**, **2**, **2'** and **3** was assessed in human cervical carcinoma HeLa, breast adenocarcinoma MCF-7 and prostate cancer PC-3 cell lines. Most active palladium derivatives **1**, **1'** were also screened for their antiproliferative effects on the non-tumorigenic human prostate RWPE-1 cell line. In addition, we evaluated the effect of the novel enantiomers of Pd(II) and Pt(II) compounds on cell adhesion and migration of the human androgen-independent prostate cancer PC-3.

Anti-proliferative studies

The *in vitro* effect of the compounds on cytotoxicity was tested by monitoring their ability to inhibit cell growth using the MTT assay and assessed as the IC_{50} values after 72 h of incubation time. The results are summarized in Table 2.
Under these conditions, pro-ligands **a·HCl**, **a'·HCl** and platinum compounds **2** and **2'** are poorly cytotoxic in all tested cell lines (IC_{50} > 100 μM). Palladium compounds are moderately cytotoxic in the cell lines assessed, with IC_{50} calculated values 2-7 times higher than those found for cisplatin. These results agree well with DNA interaction studies, where palladium compounds have shown a better binding affinity and ability to affect ds DNA structure than the platinum analogues.
Toxicity of heterometallic compound **3** is analogous to that observed for **1**, while IC_{50} calculated values for the additive dose of TDC and **1** does not show any significant difference compared to those observed for **3** in Hela and PC-3 cell lines. Due to these results, cell viability on the breast MCF-7 cancer cells was not tested in the presence of **3**.

Table 2. IC_{50} values (μM) of **a·HCl**, **a'·HCl**, cisplatin, (1*S*,4*R*)-**Ti**, enantiomers **1**, **1'**, **2** and **2'** and heterometallic complex **3** in human cervical carcinoma HeLa, breast adenocarcinoma MCF-7 and prostate cancer PC-3 cell lines (n.m. not measured).

Compound	HeLa	PC-3	MCF-7
a·HCl	> 100	> 100	> 100
a'·HCl	> 100	> 100	> 100
1	38.9 ± 3.8	25.1 ± 2.2	69.5 ± 3.7
1'	39.7 ± 4.0	27.8 ± 0.5	74.9 ± 5.5
2	> 100	> 100	> 100
2'	> 100	> 100	> 100
3	38.8 ± 1.5	23.3 ± 6.9	n.m.
(1*S*,4*R*)-**Ti**	36.4 ± 3.0	14.5 ± 3.1	> 100
TDC + 1	22.7 ± 0.44	24.5 ± 4.6	n.m.
cisplatin	11.8 ± 4.2	14.5 ± 2.5	9.8 ± 0.96

In order to assess the compounds' selectivity for cancerous cells with respect to normal cells, **1** and **1'** were also screened for their cytotoxic effects on the non-tumorigenic prostate cell line RWPE-1. The compounds **1** and **1'**, analogously to cisplatin, are as toxic to the prostate cancer PC-3 as to the non-tumorigenic prostate RWPE-1 cells (IC_{50} = 19.9 ± 1.1 cisplatin, IC_{50} = 30.6 ± 3.6 **1** and 29.6 ± 4.3 **1'**), with selectivity index (SI = IC_{50} (RWPE-1)/IC_{50} (PC-3)) of 1.4, 1.2 and 1.1 for cisplatin, **1** and **1'**, respectively.
Regarding enantiomer recognition, isomers **1** and **1'** show comparable inhibitory activities of 43-47%, 54-57% and 25-36% at concentrations of 30 μM against HeLa, PC-3 and MCF-7 cell lines, respectively. Chiral palladium(II) derivatives with antitumor effects have been reported,[115–119] but examples of a direct investigation of the influence of chirality on the anticancer activity of palladium(II) compounds are scarce. The enantiomers of the potent *in vitro* anticancer agent *trans*-[1-menthyl-4-ethyl-1,2,4-triazol-5-ylidene]$_2$Pd(OCOCF$_3$)$_2$ show nearly equal activity in MCF-7 and HeLa cell lines (IC_{50} = 0.5-0.7 μM in MCF-7 and 2.3-2.6 μM in HeLa[37]), while palladium(II) (Δ)-1,2-bis-(1H-benzimidazol-2-yl)-1,2-ethanediol enantiomer is 2-3 times more active than the (Λ)-counterpart, in the MDA-MB231 and OVCAR-8 cell lines.[120]
Some palladium compounds with tridentate pincer ligands have shown higher *in vitro* anti-tumour activity than cisplatin.[25] Some noteworthy examples are cyclometallated palladium(II) N-heterocyclic carbene compounds (IC_{50} values within the range 0.1-2.0 μM, in HeLa[121]), some thiosemicarbazone containing derivatives (IC_{50} values of 0.15 μM in MCF7[122]), and the successful terpyridine compound [PdCl(terpy)](sac)·2H$_2$O (terpy = 2,2':6',2''-terpyridine, sac = saccharinate, IC_{50} values = 1.8 μM in PC-3; 3.05 μM in MCF-7 and 5.5 in HeLa)[123,124].

Cell adhesion to collagen

Eradication of metastasis remains an unfulfilled goal.[2] Tumour metastasis is the process by which a tumour cell leaves the primary tumour, travels to a distinct site and establishes a secondary tumour. Although the mechanisms of invasion are still unclear, cell-attachment and -migration processes are recognized as key events of the "metastatic cascade".[125,126]

Within this context, we decided to evaluate the amino-oxime palladium and platinum complexes **1**, **1'** and **2**, **2'** on cell adhesion to type-I collagen, in order to determine their effect on the metastatic potential of human androgen-independent prostate cancer PC-3 cells, under conditions that did not cause cell death (compounds at 50 µM for 80 min). The disruption of cell-cell local interaction (cell adhesion) can lead to an enhanced potential for dissemination and metastatic spread of cancer cells to a secondary location.[125,126]

With this in mind, we incubated PC-3 cells in the absence or presence of 50 µM of **1**, **1'**, **2** or **2'** on a collagen plate for 80 min. The assay showed a significant increase of the cell adhesion ability after treatment with the metal compounds (**1** 29%, **1'** 20%, **2** 11%, **2'** 47% of increase) relative to untreated control cells (Fig. 6).

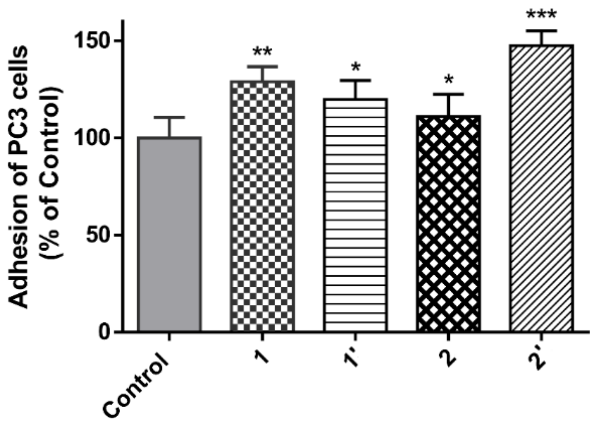

Fig. 6. Effect of **1**, **1'**, **2** and **2'** derivatives on adhesion of PC-3 cells to type-I collagen was studied after treatment with metal compounds for 80 min. Data are the mean ± S.E.M of at least four experiments. *, $P < 0.05$; ***, $P < 0.001$ *versus* Control.

Wound-healing assay

Besides changes on cell to cell interactions, metastatic cancers have other important characteristics, including the migratory and invasive activities of tumour cells. The wound-healing assay is a useful method for gauging the anti-migratory effect of drug candidates. To evaluate cell migration, we performed wound-healing assays in which a small wound area was made on the plate with a confluent monolayer of cells. After 24 h of incubation, the wound in the control wells was almost fully repopulated with migrated cells (93.0% ± 1.9 of wound area closure, Fig. 7), while the cells treated with 50 µM of palladium and platinum complexes showed a significant lower migration capability than that of control cells. Platinum enantiomers **2** and **2'** reduced migration by 11% and 8%, respectively (79.9% ± 7.8 and 84.2% ± 6.5 of wound area closure), while the palladium compounds **1** and **1'** reduced migration by 61% and 50%, respectively, (32.4% ± 6.8 and 40.8% ± 7.0 of wound area closure, respectively), relative to untreated control cells (Fig. 8). Analogous wound healing assays have been used to evaluate *in vitro* the inhibitory effect of the well-recognized *in vivo* antimetastatic metalodrug NAMI-A ([ImH][trans-$RuCl_4$(DMSO)(Im)], DMSO = dimethylsulfoxide, Im = imidazole) against the migration of a variety of cancer cell lines.[2,9,127,128] The Ru-based chemotherapeutic decrease prostatic adenocarcinoma LNCaP cell migration by ca. 30% (10 µM NAMI-A, after 24 h)[128] relative to untreated control cells. Some Pd(II) compounds have shown an influence on the cell migration and invasion potential of metastatic cancer cells. The seleno-hydantoin Pd(II) derivative inhibits migration by 60% (after 24 h of treatment) of MDA-MB-231 cells relative to control cells, at concentrations of 100 µM.[129] Potent cyctotoxic compound [PdCl(terpy)](sac)·$2H_2O$ (terpy = 2,2':6',2''-terpyridine, sac = saccharinate) is also effective in disrupting formation of MDA-MB-231 tubules on matrigel, indicative of a putative anti-invasive activity.[130]

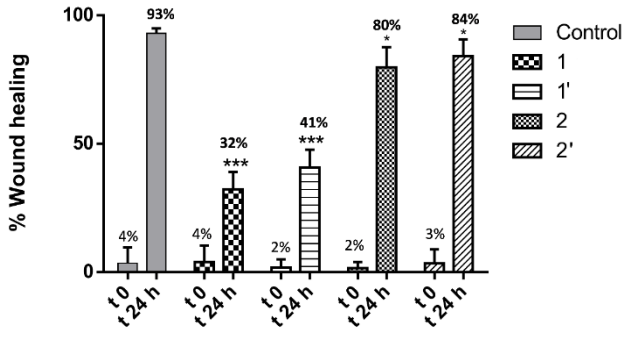

Fig. 7. Effect of **1**, **1'**, **2** and **2'** on cell migration was studied in human androgen-independent prostate cancer PC-3 cell line. Microscopic analysis of the cell-free area was carried out at 0 and 24 h after the addition of the complexes and the width of the area invaded by prostate cells was estimated. Data are the mean ± S.E.M of at least four experiments. *, $P < 0.05$; ***, $P < 0.001$ *versus* Control.

Since toxicity of **1**, **1'** is only moderate in cancer PC-3 or non-tumorigenic RWPE-1 prostatic cells, these palladium compounds could modulate both adhesion and migration activities of PC-3 cells at dose concentrations which did not cause significant cell death. On the other hand, adhesion and cell migration results ratify the compounds' adequacy for future *in vivo* assays in athymic mice.

Conclusions

The use of optically active (2-pic)amino-oxime ligands derived from natural products is a useful and inexpensive strategy to synthesize water soluble, enantiopure tricoordinated palladium and platinum compounds. The compounds were evaluated by NMR spectroscopy under physiological conditions, where single final products are detected within minutes for Pd(II) compound

and after 72 h for Pt(II) derivative. The characterization data collected for these species present at pH* = 7.4 suggests that dehydrochlorination and dimerization take place. Compound-DNA interactions have been investigated by a variety of techniques, leading to the conclusion that the metal complexes likely interact with double stranded DNA by a partial, non-classical intercalation and/or by groove binding. Palladium compounds showed better DNA binding affinity and a slight best behaviour in terms of their ability to affect the thermal and hydrodynamic properties of double stranded DNA. On the other hand, the Pd(II) compounds evaluated, **1** and **1'**, have shown medium anticancer activities against the cancer cell lines tested, with no significant differences between the two enantiomers, while Pt(II) derivatives showed poor cytotoxic profiles against the same cells. These results are in line with those obtained in the DNA interaction studies. Most importantly, adhesion and migration assays endorse the ability of **1**, **1'** to affect the metastatic phenotype of PC-3 cells *in vitro*, which makes these palladium compounds a valuable choice for further investigations.

Experimental section

General considerations

Synthesis of novel palladium and platinum complexes was performed without exclusion of moisture or air. Manipulations involving synthesis of heterometallic titanium and palladium compound were carried out at an argon/vacuum manifold using standard Schlenk techniques or in a MBraun MOD System glove-box. Solvents were dried by known procedures and used freshly distilled. (1*S*,4*R*)-, (1*R*,4*S*)-[NH(2-pic),NOH] (**a**, **a'**), corresponding adducts (1*S*,4*R*)-, (1*R*,4*S*)-[NH(2-pic)·HCl,NOH] (**a·HCl**, **a'·HCl**) and organometallic titanium compound of formula [(η^5-C_5H_5)$_2$Ti{(1*S,4R*)-κON,NH(2-pic)}Cl] ((1*S,4R*)-**Ti**) were prepared according to previous reports.[50,69,131,132] *R*- or *S*-limonene and isopentyl nitrite were reacted following the standard method described by Carman et al in 1977.[132] *R*-limonene, *S*-limonene, [(η^5-C_5H_5)$_2$TiCl$_2$] (TDC), [Pd(COD)Cl$_2$], K$_2$[PdCl$_4$], K$_2$[PtCl$_4$] and cisplatin were purchased from Sigma-Aldrich. Commercially available reagents were used without further purification. NMR spectra were recorded on a Bruker 400 Ultrashield. ^{1}H and ^{13}C chemical shifts are reported relative to tetramethylsilane. ^{15}N chemical shifts are reported relative to liquid ammonia (25 °C). Compounds concentration used were within the range 10-25 mM. Coupling constants *J* are given in Hertz. Elemental analyses were performed at our laboratories (UAH) on a LECO CHNS-932 Analyzer or, alternatively, at the Universidad Autónoma de Madrid. High Resolution Electrospray Ionization Mass Spectroscopy was performed on a Bruker MAXIS II spectrometer. IR spectra were recorded on IR FT Perkin Elmer (Spectrum 2000) spectrophotometer on KBr pellets. The pH was measured in a HANNA HI208 pHmeter in distilled water solutions. Circular Dichroism (CD) spectra were recorded on a J-715 CD spectropolarimeter (Jasco, UK) at ambient temperature (297 K). The spectra were determined at a concentration of 50 μM in water using a quartz cuvette of 0.5 cm path length, scan speed of 50 nm·min^{-1}, 1 nm band width, 0.5 nm data pitch and 1 s of response time. Optical rotations of all the compounds solutions were recorded on a Perkin Elmer 341 polarimeter, using the sodium D line (589 nm) at ambient temperature (297 K) in a quartz cell of 1 dm path length. Specific optical rotation values were calculated according to the equation $[\alpha]^{24}_D = 100\cdot\alpha_{obs}/l\cdot c$.[133] Analytical balance and volumetric pipettes (2.0 mL) were used to prepare $CHCl_3$ solutions of the compounds at concentrations within a range of 4.00-4.50 mg·mL^{-1}. UV spectra were measured at room temperature on water solutions of the compounds with a Perkin Elmer Lambda 35 spectrophotometer.

R$_N$-[Pd{(1*S*,4*R*)-κNOH,κ^{2}NH(2-pic)}Cl]Cl and *S*$_N$-[Pd{(1*R*,4*S*)-κNOH,κ^{2}NH(2-pic)}Cl]Cl (1, 1').

A solution of K$_2$[PdCl$_4$] (50 mg, 0.15 mmol) in water (2 mL) was added to a methanol (2 mL) solution of (1*S*,4*R*)- or (1*R*,4*S*)-{NOH,NH(2-pic)} (42 mg, 0.15 mmol) and stirred for 24 h at room temperature. Solvents were evaporated to dryness and chloroform (5 mL) was added. The resulting yellow suspensions were filtered to eliminate insoluble KCl and the final yellow solutions were evaporated to dryness to afford orange-yellow solids, which were washed with diethylether and dried under vacuum. Yield: 45.6 mg, 0.10 mmol, 67% (**1**) 50.3 mg, 0.11 mmol, 75% (**1'**).

Alternatively, a tetrahydrofuran (5 mL) solution of (1*S*,4*R)*- or *(1R,4S*)-{NOH,NH(2-pic)} (96.7 mg, 0.35 mmol) and [Pd(COD)Cl$_2$] (COD = 1, 5-cyclooctadiene) (100 mg, 0.35 mmol) was stirred for 24 hours at 25 °C. Evaporation of the solvent affords orange-yellow solids, which were washed with diethylether and dried under vacuum. Yield: 90 mg, 0.20 mmol, 57% (**1**) 103 mg, 0.23 mmol, 65% (**1'**).

Anal.Calcd for $C_{16}H_{23}N_3OPdCl_2\cdot 2H_2O$ (**1** or **1'**): C, 39.48; H, 5.59; N, 8.63%; Found (**1**): C, 39.66; H, 5.10; N, 8.41%. (**1'**): C, 39.09; H, 4.99; N, 8.32%. High Resolution-Electrospray Ionization Mass Spectrometry (HR-ESI-MS) **1**: m/z found (calcd) 416.0542 (416.0557) [M-Cl]$^+$ 100%. Evaporation of water solutions of **1** affords samples with the following HR-ESI-MS: m/z found (calcd) 416.0567 (416.0557) [M-Cl]$^+$ 100%. $[\alpha]^{23}_D$ (deg·dm^{-1}·dL·g^{-1}) = +127 ± 1.3 **a**, -126 ± 1.3 **a'**, -23.1 ± 1.8 **1**, +23.8 ± 1.8 **1'**. Solubility in H_2O at 24 °C (mM): 84.3. Value of pH ([2.0 mM]) in H_2O at 24 °C: 3.06. FTIR (KBr): $\tilde{\upsilon}$ 3324 (OH); 1610 (C=N). ^{1}H NMR (plus HSQC, plus HMBC, plus COSY, 400.1 MHz, 293 K, chloroform-*d*$_1$): δ 10.61 (br, 1H, -NH), 8.95 (1H, NOH), 8.43, 7.92, 7.59, 7.33 (all m, each 1H, -NC$_5$H$_4$), 5.06, 4.72 (both s, each 1H, =CH$_2$), 4.53 (dd, 1H, J_{HH}= 9 Hz, J_{HH}= 15 Hz, -CH$_2$-C$_5$NH$_4$), 4.45 (dd, 1H, J_{HH}= 5 Hz, J_{HH}= 15 Hz, -CH$_2$-C$_5$NH$_4$), 3.37 (d, 1H, J_{HH}= 17 Hz, -CH$_2^3$), 2.80 (m, 1H, -CH$_2^6$), 2.77 (m, 1H, -CH-C=), 2.28 (dd, 1H, J_{HH}= 6 Hz, J_{HH}= 17 Hz, -CH$_2^3$), 2.00 (m, 1H, -CH$_2^5$), 1.88 (s, 3H, NC-CH$_3$), 1.85 (m, 1H, -CH$_2^6$), 1.70 (s, 3H, CH$_3$C=), 1.68 (m, 1H, -CH$_2^5$). ^{13}C- NMR (plus APT, plus gHSQC, plus HMBC, 100.6 MHz, 293 K, chloroform-*d*$_1$):δ 175.9 (+, Cq=N), 165.7 (+, C$_{ipso}$NC$_5$H$_4$), 143.4 (+, =Cq-Me), 150.5, 140.5, 124.1, 122.6 (–, NC$_5$H$_4$), 113.3 (+, =CH$_2$), 69.6 (+, Cq-NH), 51.9 (+, -***C***H$_2$-C$_5$NH$_4$), 38.3 (–, -CH^4), 31.2 (+, -CH$_2^6$), 29.1 (+, -CH$_2^3$), 24.3 (+, -CH$_2^5$), 23.9 (–, *C*H$_3$-CNH), 21.6 (–, *C*H$_3$-C=). ^{15}N NMR (gHMBC, 40.5 MHz, 293 K, chloroform-*d*$_1$): δ 258.2 (C=NOH), 220.7 (NC$_5$H$_4$), 61.2 (NHpic). ^{1}H NMR (400.1 MHz, 293 K, water-*d*$_2$, pH* = 2.3): δ 8.55, 8.19,

7.69, 7.61 (all m, each 1H, -NC_5H_4), 5.12 (s, 1H, =CH_2), 5.07 (d, 1H, J_{HH} = 16 Hz, C$\underline{H_2}$-C_5NH_4), 4.73 (s, 1H, =CH_2), 4.26 (d, 1H, J_{HH} = 16 Hz, -C$\underline{H_2}$-C_5NH_4), 3.58 (d, 1H, J_{HH} = 20 Hz, -CH_2^3), 2.83 (br, 1H, -CH-C=), 2.68 (dd, 1H, J_{HH} = 4 Hz, J_{HH} = 20 Hz, -CH_2^3), 2.18 (m, 2H, -CH_2^{5+6}), 2.14 (s, 3H, NC-CH_3), 2.01 (m, 2H, -CH_2^{5+6}), 1.85 (s, 3H, CH_3C=). ^{13}C- NMR (plus APT, plus gHSQC, plus HMBC, 100.6 MHz, 293 K, water-d_2, pH* = 2.3): δ 181.4 (+, Cq=N), 165.5 (+, $C_{ipso}NC_5H_4$), 146.7 (+, =Cq-Me), 150.2, 141.5, 124.9, 122.9 (–, NC_5H_4), 111.4 (+, =CH_2), 69.0 (+, Cq-NH), 51.5 (+, -***C***H_2-C_5NH_4), 38.8 (–, -CH^4), 31.9 (+, -CH_2^6), 29.5 (+, -CH_2^3), 24.8 (+, -CH_2^5), 23.4 (–, *C*H_3-CNH), 21.4 (–, *C*H_3-C=). ^{15}N NMR (gHMBC, 40.5 MHz, 293 K, water-d_2, pH* = 2.3): δ 260.9 (C=NOH), 216.5 (NC_5H_4), 58.0 (NHpic).

Characterization data of palladium species present at pH = 7.4.*

High Resolution Electrospray Ionization Mass Spectrometry (HR-ESI-MS): m/z found (calcd) 379.0784 (379.0802) $[2M-2Cl-2H]^{2+}$, 100%.

^{1}H NMR (400.1 MHz, 293 K, water-d_2, pH* = 7.4): δ 8.12, 8.06, 7.53, 7.48 (all m, each 1H, -NC_5H_4), 4.99 (s, 1H, =CH_2), 4.72 (overlapped, 2H, =CH_2+-CH_2-C_5NH_4), 4.04 (d, 1H, J_{HH}= 17 Hz, -CH_2-C_5NH_4), 3.51 (d, 1H, J_{HH}= 17 Hz, -CH_2^3), 2.67 (m, 1H, -CH-C=), 2.41 (dd, 1H, J_{HH}= 6 Hz, J_{HH}= 17 Hz, -CH_2^3), 2.01 (m, 2H, -CH_2^{5+6}), 1.96 (s, 3H, NC-CH_3), 1.84 (m, 1H, -CH_2^{5+6}), 1.76 (s, 3H, CH_3C=). ^{13}C- NMR (plus APT, plus gHSQC, plus HMBC, 100.6 MHz, 293 K, water-d_2 pH* = 7.4):δ 173.1 (+, Cq=N), 164.5 (+, $C_{ipso}NC_5H_4$), 147.4 (+, =Cq-Me), 147.4, 141.1, 124.2, 122.5 (–, NC_5H_4), 110.3 (+, =CH_2), 68.0 (+, Cq-NH), 50.2 (+, -***C***H_2-C_5NH_4), 38.7 (–, -CH^4), 31.6 (+, -CH_2^6), 28.9 (+, -CH_2^3), 23.9 (+, -CH_2^5), 23.2 (–, *C*H_3-CN), 21.3 (–, *C*H_3-C=). ^{15}N NMR (gHMBC, 40.5 MHz, 293 K, water-d_2, pH* = 7.4): δ 296.3 (C=NOH), 225.8 (NC_5H_4), 51.1 (NHpic).

R_N-[Pt{(1*S*,4*R*)-κNOH,κ²NH(2-pic)}Cl]Cl or S_N-[Pt{(1*R*,4*S*)-κNOH,κ²NH(2-pic)}Cl]Cl (2, 2').

A solution of $K_2[PtCl_4]$ (80 mg, 0.19 mmol) in water (2 mL) was added to a methanol (2 mL) solution of (1*S*,4*R*)- or (1*R*,4*S*)-{NOH,NH(2-pic)} (53 mg, 0.19 mmol) and stirred for 24 h at room temperature. Green-yellow reaction mixtures were obtained thereafter. Solvents were evaporated and $CHCl_3$ was added, final solutions were filtered to separate the insoluble KCl and the resulting yellow solutions were dried under vacuum to afford green-yellow solids. Yield: 73 mg, 0.13 mmol, 70% (**2**) 76 mg, 0.14 mmol 73% (**2'**). Anal.Calcd for $C_{16}H_{23}N_3OPtCl_2{\cdot}2H_2O$ (**2** or **2'**): C, 33.40; H, 4.73; N, 7.30; Found (**2**): C, 33.38; H, 4.28; N, 6.98. (**2'**): C, 33.04; H, 4.33; N, 7.18. High Resolution Electrospray Ionization Mass Spectrometry (HR-ESI-MS) **2**: m/z found (calcd) 504.1139 (504.1166) $[M-Cl]^+$ 100%. **2'**: m/z found (calcd) 504.1149 (504.1166) $[M-Cl]^+$ 100%. Evaporation of water solutions of **2** affords samples with the following HR-ESI-MS: m/z found (calcd) 504.1157 (504.1166) $[M-Cl]^+$ 100%; 467.1398 (467.1402) $[2M-2Cl-2H]^{2+}$ 8%. $[\alpha]^{23}_D$ (deg·dm^{-1}·dL·g^{-1}) = +127 ± 1.3 **a**, -126 ± 1.3 **a'**, -32.9 ± 1.8 **2**, +33.1 ± 1.8 **2'**. Solubility in H_2O at 24 °C (mM): 13.3. Value of pH ([2.0 mM]) in H_2O at 24 °C: 4.72. FTIR (KBr): ῡ 3336 (OH); 1613 (C=N). ^{1}H NMR (plus HSQC, plus HMBC, plus COSY, 400.1 MHz, 293 K, chloroform-d_1): δ 10.51 (1H, -NH), 9.23 (br, 1H, NOH), 8.66, 7.97, 7.61, 7.32 (all m, each 1H, -NC_5H_4), 5.02, 4.73 (both s, each 1H, =CH_2), 4.63, 4.43 (both d, each 1H, J_{HH}= 15 Hz, -CH_2-C_5NH_4), 3.37 (d, 1H, J_{HH}= 17 Hz, -CH_2^3), 2.82 (m, 1H, -CH_2^6), 2.57 (m, 1H, -CH-C=), 2.23 (dd, 1H, J_{HH}= 6 Hz, J_{HH}= 17 Hz, -CH_2^3), 1.93 (overlapped, 2H, -CH_2^{5+6}), 1.84 (s, 3H, NC-CH_3), 1.70 (m, 1H, -CH_2^5), 1.72 (s, 3H, CH_3C=). ^{13}C-NMR (plus APT, plus gHSQC, plus HMBC, 100.6 MHz, 293 K, chloroform-d_1): δ 175.4 (+, Cq=N), 167.5 (+, $C_{ipso}NC_5H_4$), 144.1 (+, =Cq-Me), 149.7, 140.3, 124.6, 123.1 (–, NC_5H_4), 113.3 (+, =CH_2), 70.6 (+, Cq-NH), 52.0 (+, -***C***H_2-C_5NH_4), 38.8 (–, -CH^4), 31.9 (+, -CH_2^6), 29.0 (+, -CH_2^3), 24.7 (+, -CH_2^5), 23.5 (–, *C*H_3-CNH), 22.0 (–, *C*H_3-C=). ^{15}N NMR (gHMBC, 40.5 MHz, 293 K, chloroform-d_1): δ 245.0 (C=NOH), 208.2 (C_5NH_4), 48.8 (NHpic). ^{1}H NMR (400.1 MHz, 293 K, water-d_2, pH* = 3.0): δ 8.73, 8.15, 7.62, 7.52 (all m, each 1H, -NC_5H_4), 5.03 (s, 1H, =CH_2), 4.90 (d, 1H, J_{HH} = 16 Hz, C$\underline{H_2}$-C_5NH_4), 4.64 (s, 1H, =CH_2), 4.31 (d, 1H, J_{HH} = 16 Hz, -C$\underline{H_2}$-C_5NH_4), 3.52 (d, 1H, J_{HH} = 20 Hz, -CH_2^3), 2.72 (br, 1H, -CH-C=), 2.49 (dd, 1H, J_{HH} = 4 Hz, J_{HH} = 20 Hz, -CH_2^3), 2.14 (m, 2H, -CH_2^{5+6}), 1.96 (s, 3H, NC-CH_3), 2.01 (m, 2H, -CH_2^{5+6}), 1.77 (s, 3H, CH_3C=). ^{13}C- NMR (plus APT, plus gHSQC, plus HMBC, 100.6 MHz, 293 K, water-d_2, pH* = 3.0): δ 181.3 (+, Cq=N), 166.3 (+, $C_{ipso}NC_5H_4$), 148.7 (+, =Cq-Me), 149.0, 141.0, 124.4, 122.7 (–, NC_5H_4), 110.7 (+, =CH_2), 70.0 (+, Cq-NH), 51.5 (+, -***C***H_2-C_5NH_4), 38.7 (–, -CH^4), 31.7 (+, -CH_2^6), 29.5 (+, -CH_2^3), 23.4 (+, -CH_2^5), 22.1 (–, *C*H_3-CNH), 21.0 (–, *C*H_3-C=). ^{15}N NMR (gHMBC, 40.5 MHz, 293 K, water-d_2, pH* = 3.0): δ 243.5 (C=NOH), 200.9 (C_5NH_4), 44.8 (NHpic).

Characterization data of platinum species present at pH = 7.4 (72 h after dilution)*

High Resolution Electrospray Ionization Mass Spectrometry (HR-ESI-MS): m/z found (calcd) 467.1387 (467.1402) $[2M-2Cl-2H]^{2+}$, 100%.

^{1}H NMR (400.1 MHz, 293 K, water-d_2, pH* = 7.4): δ 8.23, 8.03, 7.49, 7.41 (all m, each 1H, -NC_5H_4), 4.87 (s, 1H, =CH_2), 4.60 (overlapped, 2H, =CH_2 + CH_2-C_5NH_4), 4.03 (d, 1H, J_{HH}= 16 Hz, -C$\underline{H_2}$-C_5NH_4), 3.45 (d, 1H, J_{HH} = 16 Hz, -CH_2^3), 2.59 (m, 1H, -CH-C=), 2.34 (dd, 1H, J_{HH}= 6 Hz, J_{HH}= 16 Hz, -CH_2^3), 1.90 (overlapped, 2H, -CH_2^{6+5}), 1.81 (overlapped, 5H, NC-CH_3 + -CH_2^{6+5}), 1.66 (s, 3H, CH_3C=). ^{13}C- NMR (plus APT, plus gHSQC, plus HMBC, 100.6 MHz, 293 K, water-d_2, pH* = 7.4):δ 173.8 (+, Cq=N), 165.8 (+, $C_{ipso}NC_5H_4$), 147.8 (+, =Cq-Me), 146.9, 141.2, 124.7, 123.1 (–, NC_5H_4), 110.9 (+, =CH_2), 70.2 (+, Cq-NH), 51.1 (+, -***C***H_2-C_5NH_4), 39.1 (–, -CH^4), 31.9 (+, -CH_2^6), 28.4 (+, -CH_2^3), 24.0 (+, -CH_2^5), 22.5 (–, *C*H_3-CN), 21.7 (–, *C*H_3-C=). ^{15}N NMR (gHMBC, 40.5 MHz, 293 K, water-d_2, pH* = 7.4): δ 274.4 (C=NOH), 206.7 (NC_5H_4), 30.4 (NHpic).

R_N-[Pd{(1*S*,4*R*)-κNOH,κ²NH(2-pic)}Cl]PF_6 (1·PF_6).

A dichloromethane (5 mL) solution of **1** (20 mg, 0.044 mmol) and KPF_6 (8.2 mg, 0.044 mmol) was stirred for 24 hours at 25 °C. The resulting suspension was filtered to separate the insoluble KCl and the final yellow solution was dried under vacuum to afford a yellow solid. Yield: 14.5 mg, 0.026 mmol, 59% (**1·PF_6**). ^{1}H NMR (400.1 MHz, 293 K, diclorometane-d_2): δ 8.97 (1H, NOH), 8.45, 8.00, 7.51, 7.43 (all m, each 1H, -NC_5H_4), 6.84 (br, 1H, -NH), 5.01, 4.65 (both s, each 1H, =CH_2), 4.70 (d, 1H, J_{HH}= 10 Hz, -CH_2-C_5NH_4), 4.24 (dd, 1H, J_{HH}= 5 Hz, J_{HH}= 16 Hz, -CH_2-C_5NH_4), 3.42 (d, 1H, J_{HH}= 17 Hz, -CH_2^3), 2.65 (m, 1H, -CH-C=), 2.35 (dd, 1H, J_{HH}= 6 Hz, J_{HH}= 17 Hz, -CH_2^3), 2.09 (m, 1H, -CH_2^5), 1.96 (m, 2H, -CH_2^6), 1.91 (s, 3H, NC-CH_3), 1.80 (m, 1H, -CH_2^5), 1.74 (s, 3H, CH_3C=). ^{15}N NMR (gHMBC, 40.5 MHz, 293 K, diclorometane-

d$_2$): δ 258.3 (C=NOH), 221.3 (NC_5H_4), 58.3 (NHpic). ^{19}F NMR (376.5 MHz, 293 K, dichloromethane-*d*$_2$): δ = –71.8 (d, $J_{P,F}$ = 715 Hz, PF_6) ppm. ^{31}P NMR (161.9 MHz, 293 K, CD_2Cl_2): δ = –144.4 (sept, $J_{P,F}$ = 715 Hz, PF_6).

R_N-[Pt{(1*S*,4*R*)-κNOH,κ^{2}NH(2-pic)}Cl]PF_6 (2·PF_6).

A similar procedure as that described for **1·PF_6** was followed, starting from **2** (20 mg, 0.037 mmol) and KPF_6 (6.8 mg, 0.37 mmol). Yield: 13.4 mg, 0.021 mmol, 56% (**2·PF_6**).
^{1}H NMR (400.1 MHz, 293 K, dichloromethane-*d*$_2$): δ 9.17 (br, 1H, NOH), 8.69, 8.05, 7.56, 7.42 (all m, each 1H, -NC_5H_4), 7.92 (1H, -NH), 4.96, 4.61 (both s, each 1H, =CH_2), 4.50 (m, 1H, -CH_2-C_5NH_4), 4.40 (dd, 1H, J_{HH}= 5 Hz, J_{HH}= 16 Hz, -CH_2-C_5NH_4), 3.37 (d, 1H, J_{HH}= 17 Hz, -CH_2^3), 2.61 (m, 1H, -CH-C=), 2.26 (overlapped, 2H, -CH_2^{3+6}), 1.99 (m, 1H, -CH_2^5), 1.92 (m, 1H, -CH_2^6), 1.84 (s, 3H, NC-CH_3), 1.77 (m, 1H, -CH_2^5), 1.73 (s, 3H, CH_3C=). ^{15}N NMR (gHMBC, 40.5 MHz, 293 K, dichloromethane-*d*$_2$): δ 244.1 (C=NOH), 205.6 (NC_5H_4), 48.0 (NHpic). ^{19}F NMR (376.5 MHz, 293 K, dichloromethane-*d*$_2$): δ = –66.4 (d, $J_{P,F}$ = 713 Hz, PF_6) ppm. ^{31}P NMR (161.9 MHz, 293 K, dichloromethane-*d*$_2$): δ = –144.6 (sept, $J_{P,F}$ = 713 Hz, PF_6).

[(η^5-C_5H_5)$_2$Ti(1*S*,4*R*)-κON,(*R*)κ^{2}NH(2-pic)(PdCl)]Cl (3).

A dichloromethane (10 mL) solution of [(η^5-C_5H_5)$_2$Ti{(1*S*,4*R*)-κON,NH(2-pic)}] ((1*S*,4*R*)-**Ti**)[50] (80 mg, 0.16 mmol) and $[Pd(COD)Cl_2]$ (45.7 mg, 0.16 mmol) was stirred for 2 h at room temperature. The resulting orange suspension was dried under vacuum to give an orange solid, which was identified as derivative **3**. Yield: 82 mg, 0.12 mmol, 77%. Anal.Calcd for $C_{26}H_{32}N_3OPdTiCl_3$: C, 47.08; H, 4.87; N, 6.34; Found: C, 46.56; H, 4.25; N, 6.38. Solubility in H_2O at 24 °C (mM): 3.02. Value of pH ([2.0 mM]) in H_2O at 24 °C: 3.87. ^{1}H NMR (plus HSQC, plus HMBC, plus COSY, 400.1 MHz, 293 K, chloroform-*d*$_1$): δ 10.89 (1H, -NH), 8.73, 7.87, 7.46, 7.32 (all m, each 1H, -NC_5H_4), 6.76, 6.54 (s, each 5H, -C_5H_5), 5.03, 4.79 (both s, each 1H, =CH_2), 4.39 (m, 2H, -CH_2-C_5NH_4), 3.21 (dd, 1H, J_{HH}= 5 Hz, J_{HH}= 19 Hz, -CH_2^3), 2.82 (m, 1H, -CH_2^6), 2.44 (m, 1H, -CH-C=), 2.30 (dd, 1H, J_{HH}= 7 Hz, J_{HH}= 19 Hz, -CH_2^3), 2.04 (s, 3H, NC-CH_3), 1.90 (m, 1H, -CH_2^5), 1.79 (m, 1H, -CH_2^6), 1.72 (s, 3H CH_3C=), 1.66 (m, 1H, -CH_2^5). ^{13}C- NMR (plus APT, plus gHSQC, plus HMBC, 100.6 MHz, 293 K, chloroform-*d*$_1$): δ 176.2 (+, Cq=N), 166.2 (+, $C_{ipso}NC_5H_4$), 150.5 (+, =Cq-Me), 144.4, 140.1, 123.9, 122.4 (–, NC_5H_4), 120.1, 119.2 (–, C_5H_5), 113.1 (+, =CH_2), 67.2 (+, Cq-NH), 51.4 (+, -***C***H_2-C_5NH_4), 38.3 (–, -CH^4), 31.6 (+, -CH_2^6), 31.3 (+, -CH_2^3), 26.4 (–, *C*H_3-CNH), 25.1 (+, -CH_2^5), 21.6 (–, *C*H_3-C=). ^{15}N NMR (gHMBC, 40.5 MHz, 293 K, chloroform-*d*$_1$): δ 301.4 (C=NOH), 220.9 (NC_5H_4), 60.7 (NHpic).

[(η^5-C_5H_5)$_2$Ti(1*S*,4*R*)-κON,(*R*)κ^{2}NH(2-pic)(PdCl)]PF_6 (3·PF_6).

A dichloromethane (5 mL) solution of **3** (10 mg, 0.015 mmol) and KPF_6 (2.8 mg, 0.015 mmol) was stirred for 24 hours at 25 °C. The solution was filtered to separate the insoluble KCl and the resulting orange solution was dried under vacuum to afford an orange solid. Yield: 8.7 mg, 0.011 mmol, 75%.
^{1}H NMR (400.1 MHz, 293 K, dichloromethane-*d*$_2$):):δ 8.72, 7.97, 7.50, 7.41 (all m, each 1H, -NC_5H_4), 7.31 (br, 1H, -NH), 6.66, 6.57 (s, each 5H, C_5H_5) 5.99, 4.65 (both s, each 1H, =CH_2), 4.60 (m, 1H, -CH_2-C_5NH_4), 4.19 (dd, 1H, J_{HH}= 7 Hz, J_{HH}= 16 Hz, -CH_2-C_5NH_4), 3.33 (d, 1H, J_{HH}= 18 Hz, -CH_2^3), 2.53 (m, 1H, -CH-C=), 2.25 (dd, 1H, J_{HH}= 6 Hz, J_{HH}= 18 Hz, -CH_2^3), 2.15 (m, 1H, -CH_2^6), 2.03 (s, 3H, NC-CH_3), 1.90 (overlapped, 3H, -CH_2^{5+6}), 1.72 (s, 3H, CH_3C=). ^{15}N NMR (gHMBC, 40.5 MHz, 293 K, dichloromethane-*d*$_2$): δ 303.4 (C=NOH), 219.8 (NC_5H_4), 56.9 (NHpic).^{19}F NMR (282.4 MHz, 293 K, dichloromethane-*d*$_2$): δ = –66.0 (d, $J_{P,F}$ = 714 Hz, PF_6) ppm. ^{31}P NMR (161.9 MHz, 293 K, dichloromethane-*d*$_2$): δ = –144.5 (sept, $J_{P,F}$ = 714 Hz, PF_6).

Time- and pH-dependant NMR experiments

The compounds were dissolved in 2000 µL of water-*d*$_2$ and time-dependent ^{1}H NMR spectra of 500 µL aliquots of final solutions were carried out. Phosphate buffered saline solution (PBS) or Phosphate buffered solution (PB) were prepared according to Cold Spring Harbor Protocols (http://cshprotocols.cshlp.org/content/2006/1/pdb.rec8247) using NaCl, KCl, Na_2HPO_4 and KH_2PO_4 in water-*d*$_2$ or Na_2HPO_4 and KH_2PO_4 in water-*d*$_2$. Adjustment of pH* (pH* = pHmeter reading in water-*d*$_2$) was carried out using a solution of DCl (0.01M) or NaOD (0.01M) in water-*d*$_2$, with the help of a HANNA HI208 pHmeter. Palladium and platinum compounds were then dissolved in 2000 µL of the freshly prepared PBS or PB solution, final pD measured (7.30-7.38) and time-dependent ^{1}H NMR spectra of 500 µL aliquots of final solutions were carried out at 25 °C. Alternatively, the compounds were dissolved in 2000 µL of water-*d*$_2$ and final pH* adjusted to desired values using a solution of DCl (0.01M) or NaOD (0.01 M) in water-*d*$_2$, and time-dependent ^{1}H NMR spectra of 500 µL aliquots of final solutions were carried out.

n-Octanol–Water Partition Coefficients

The n-octanol–water partition coefficient was measured by using the shake-flask method.[100] Distilled water and n-octanol were stirred together for 72 h at 25 °C, to promote saturation of both phases. The solvents were separated and freshly used. Aliquots of stock solutions (1.5 mM) of **1** and (150 µM) of **2** in the n-octanol saturated aqueous phase were added to equal volumes of water-saturated n-octanol and shaken on a mechanical shaker for 1 h. The resultant biphasic solution was centrifuged to separate the layers, and UV/Vis absorption spectra of both solutions were registered in both phases in a Perkin Elmer Lambda 35 UV/Vis spectrophotometer at 372 nm (**1**) and 270 nm (**2**) and compared with a calibration curve to obtain the compound concentration of **1** and **2** in both phases. logP was defined as the logarithm of the ratio [Pd]octanol/[Pd]water or [Pt]octanol/[Pt]water, respectively; values reported are the means of three separate experiments.

DNA interaction studies

Equilibrium Dialysis

Duplex DNA from calf thymus (CT DNA), (Deoxyribonucleic acid, Activated, Type XV) was directly purchased from Sigma Aldrich and used as provided. Dialysis membranes (Spectra/Por® molecular porous membrane tubing, MWCO: 3.5–5.0 kDa; 6.4 mm diameter) were purchased from Spectrum Laboratories Inc. Aqueous solutions of surfactant sodium dodecyl sulfate (SDS)

(10%) were purchased from Sigma Aldrich. A 10 mM phosphate buffer NaH_2PO_4/Na_2HPO_4, pH = 7.2 buffer was used in this experiment. DNA solutions in phosphate buffer were prepared at 75 μM monomeric unit (m.u.) concentrations, in bp.

Dialysis bags, previously washed with milli-Q water, were filled with 75 μM (m.u.) of duplex DNA (200 μL each bag) and placed in a beaker containing 225 mL of ca. 5 μM solution of the tested compound. The beaker was covered with parafilm and aluminium foil and allowed to equilibrate during 24 h at room temperature with continuous stirring. Experiments were run, at least, in triplicate. Once the dialysis process had been completed, the solutions from each dialysis bag were transferred to Eppendorf tubes. The content of each bag was then mixed with an aqueous detergent solution (10%) to reach a SDS concentration of 1% (v/v). The concentrations of free compound in the dialysate solution and compound in the dialysis bags were determined by absorbance measurements using the extinction coefficients of the metal complexes (determined previously in the presence and in the absence of the detergent) and apparent association constants were calculated.[103]

DNA FRET melting assay

DNA melting assays were performed using a quantitative PCR kit ABI PRISM® 7000 Sequence Detection System (Applied Biosystems) in a 96-well plate format (96-Well Optical MicroAmp® Reaction Plate, Applied Biosystems, Life Technologies Corporation). The oligonucleotide sequence employed in this experiment, F10T (5'-FAM- TAT AGC TA TA /sp18/ TA TA GCT ATA-TAMRA-3') was synthesized, HPLC-purified and desalted by IDT. FAM is 6-carboxyfluorescein and TAMRA is carboxytetramethylrhodamine. The buffer system used in this experiment was 10 mM sodium cacodylate, 100 mM LiCl, (pH = 7.3).

First, the duplex-forming oligonucleotide was dissolved in water (Biotechnology Performance Certified, BPC grade) and a 50 μM stock solution was prepared, which was then diluted to 0.5 μM. Then, the diluted DNA solution was mixed with the working buffer (2X) and water (BPC grade). The DNA solution was heated at 90 °C for 10 min, cooled down slowly for 3 h and left at 4 °C overnight. Compounds to be tested were dissolved in water and approximately 1 mM stock solutions were prepared. The exact concentrations were checked by UV-visible. Stock solutions were then diluted with buffer to obtain 50 μM solutions of each compound. In a 96-well microplate, DNA solutions were mixed with solutions of tested compound and buffer to reach a total volume of 50 μL with a F10T concentration of 0.2 μM and a compound concentration ranging between 1 and 10 μM.

The melting protocol consisted of an incubation for 5 min at 24 °C, followed by a temperature ramp with a heating rate of 1 °C/min. Conversely, the reverse folding process consisted on incubation at 96°C for 5 min, followed by a temperature ramp with a cooling rate of -1 °C/min. Fluorescence values corresponding to the fluorophore FAM at wavelength of 516 nm (after excitation at 492 nm) were collected at each degree of temperature. Afterwards, the fluorescence data were normalized, plotted against temperature (°C) at each compound concentration, and melting temperatures (Tm) values were estimated as $T_{1/2}$.

Viscosity titrations

Duplex DNA from CT (Deoxyribonucleic acid, Activated, Type XV) was purchased from Sigma Aldrich and used as provided. A 10 mM phosphate buffer (NaH_2PO_4/Na_2HPO_4) pH = 7.2 was used. The viscosity measurements were performed in a Visco System AVS 470 at 25.00 ± 0.01 °C, using a microUbbelohde (K = 0.01) capillary viscometer. 6 mL of DNA solution (0.4 mM in nucleotides) in phosphate buffer were equilibrated for 20 min at 25.00 °C and then 20 flow times were registered. Small aliquots (25–40 μL) of solutions of metal complexes (1.5-1.7 mM) were added to the same DNA solution. Before each flow time registration, the solutions were equilibrated for 20 min to 25.00 °C and then 20 flow times were measured. With the averaged time of the different flow time measurements and the viscometer constant, the viscosities (μ) for each point were calculated. The viscosity results were plotted as $(\mu/\mu_0)^{1/3}$, where μ_0 represents the DNA solution viscosity in the absence of the ligand, versus (r), representing the ratio [ligand]/[DNA].

***In vitro* cell studies**

Cell culture

The human cervical carcinoma cell line HeLa, the human breast adenocarcinoma cell line MCF-7, the human prostate cancer cell line PC-3 and non-tumorigenic prostate cells line RWPE-1 were obtained from the American Type Culture Collection (Manassas, VA). MCF-7 cells were grown routinely in DMEM (Dulbecco's modified Eagle's medium), RWPE-1 in DMEM/F12 (Dulbecco's Modified Eagle Medium: Nutrient Mixture F-12) and PC-3 and HELA cells in RPMI-1640 (Roswell Park Memorial Institute), supplemented with 5% fetal bovine serum (FBS), 200 $U \cdot mL^{-1}$ penicillin, 100 μg·mL-1 streptomycin and 2 mM L-glutamine (all from Sigma-Aldrich). The culture was performed in a humidified 5% CO_2 environment at 37 °C. After the cells reached 70–80% confluence, they were washed with PBS, detached with 0.25% trypsin/0.2% EDTA and seeded at 30,000–40,000 $cells \cdot cm^{-2}$. The culture medium was changed every 3 days. Cultures were maintained in a humidified atmosphere of 95% air: 5% CO_2 at 37 °C. Adherent cells were allowed to attach for 48 h prior to addition of compounds.

MTT Toxicity Assays

For toxicity assays, cells (approximately 5×10^3 cells mL^{-1}) were seeded in flat-bottom 96-well plates (100 μL/well) in complete medium. Adherent cells were allowed to attach for 48 h prior to addition of cisplatin or tested compounds. Stock solutions of ammonium-oxime pro-ligand were freshly prepared in 1% of dimethyl sulfoxide (DMSO) in medium, while cisplatin and new compounds were freshly dissolved in corresponding medium. The stock solutions were then diluted in complete medium and used for sequential dilutions to desired concentrations. The final concentration of DMSO in the cell culture medium did not exceed 0.1%. Control groups with and without DMSO (0.1%) were included in the assays. Compounds were then added at different concentrations in quadruplicate. Cells were incubated

with compounds for 72 h, and then cell proliferation was determined by the MTT-reduction method. Briefly, 10 µL/well of [3-(4,5-dimethylthiazol-2-yl)-2,5-diphenyltetrazolium bromide] (MTT) (5 mg·mL-1 in PBS) was added, and plates were incubated for 3–4 h at 37 °C. After that time, the culture medium was removed, and the purple formazan crystals formed by the mitochondrial dehydrogenase and reductase activity of vital cells were dissolved in DMSO. The optical density, directly proportional to the number of surviving cells, was quantified at 570 nm (background correction at 630 nm) using a multiwell plate reader and the fraction of surviving cells was calculated from the absorbance of untreated control cells. The IC_{50} value indicates the concentration needed to inhibit the biological function of the cells by half and is presented as a mean ± SD of three independent experiments, each comprising four microcultures per concentration level.

Cell adhesion assay

Concentrated type-I collagen solution (8 µg/cm^2) was diluted in 10 mM glacial acetic acid and coated onto 96-well plates for 1 h at 37°C. Plates were washed twice with PBS (pH 7.4). PC-3 cells were harvested with 0.25% trypsin/0.2% EDTA and collected by centrifugation. They were suspended in RPMI medium/0.1% (w/v) bovine serum albumin (BSA) (pH 7.4). The cells were incubated in either the absence or presence of the complexes for 30 min. Then, cells were plated at 2.5 x 10^4 cells per 100 µl. The assay was terminated at indicated time intervals by aspiration of the wells. Cell adhesion was quantified by MTT colorimetric assay as described above. Control samples (in the absence of metal compounds) were averaged and assigned a value of 100%.

Wound-healing assay

PC-3 cells were seeded in 24-well plates at a density of 1.5 x 10^{5}cells in complete media (10% FBS and 1% penicillin/streptomycin/amphoterycin B), and then grown to confluence for 24 h. A small wound area was made with a scraper in the confluent monolayer. The cells were then incubated in either the absence or presence of the complexes. Four representative fields of each wound were captured using a Nikon Diaphot 300 inverted microscopy at different times (0–24 h). Wound areas of samples at time 0 were averaged and assigned a value of 100%.

Data analysis

Results were subjected to computer-assisted statistical analysis using One-Way Analysis of Variance ANOVA, Bonferroni´s post-test, and Student´s t-test. Data are shown as the means of individual experiments and presented as the mean ± S.E.M (Standard error deviation). Differences of $P < 0.05$ were considered to be significantly different from the controls.

Conflicts of interest

There are no conflicts to declare.

Acknowledgements

Financial support from Comunidad Autónoma de Madrid (CAM, I3 Program) and the Universidad de Alcalá (UAH, Projects UAH-AE-2017-2, CCG2017-EXP019, CCG2018-EXP024, CCG2015/BIO-010) is acknowledged. I.C.A. and E.T.R. are grateful to UAH and MEC for their fellowships.

Notes and references

1 N. J. Wheate, S. Walker, G. E. Craig and R. Oun, *Dalt. Trans.*, 2010, **39**, 8113.
2 A. Bergamo and G. Sava, *Chem. Soc. Rev.*, 2015, **44**, 8818–8835.
3 M. Hanif and C. G. Hartinger, *Future Med. Chem.*, 2018, **10**, 615–617.
4 L. Bai, C. Gao, Q. Liu, C. Yu, Z. Zhang, L. Cai, B. Yang, Y. Qian, J. Yang and X. Liao, *Eur. J. Med. Chem.*, 2017, **140**, 349–382.
5 C. S. Allardyce and P. J. Dyson, *Dalt. Trans.*, 2016, **45**, 3201–3209.
6 R. G. Kenny, S. W. Chuah, A. Crawford and C. J. Marmion, *Eur. J. Inorg. Chem.*, 2017, **12**, 1596–1612.
7 K. Laws and K. Suntharalingam, *ChemBioChem*, 2018, **19**, 2246–2253.
8 B. S. Murray, M. V Babak, C. G. Hartinger and P. J. Dyson, *Coord. Chem. Rev.*, 2016, **306**, 86–114.
9 E. Alessio, *Eur. J. Inorg. Chem.*, 2017, **12**, 1549–1560.
10 J. Reedijk, *Eur. J. Inorg. Chem.*, 2009, **10**, 1303–1312.
11 D. Wang and S. J. Lippard, *Nat. Rev. Drug Discov.*, 2005, **4**, 307–320.
12 V. Brabec, O. Hrabina and J. Kasparkova, *Coord. Chem. Rev.*, 2017, **351**, 2–31.
13 S. Komeda, *Metallomics*, 2011, **3**, 650–655.
14 T. C. Johnstone, K. Suntharalingam and S. J. Lippard, *Chem. Rev.*, 2016, **116**, 3436–3486.
15 J. J. Wilson and S. J. Lippard, *Chem. Rev.*, 2014, **114**, 4470–4495.
16 M. Trajkovski, E. Morel, F. Hamon, S. Bombard, M.-P. Teulade-Fichou and J. Plavec, *Chem. Eur. J.*, 2015, **21**, 7798–7807.
17 J. E. Reed, A. J. P. White, S. Neidle and R. Vilar, *Dalt. Trans.*, 2009, 2558–2568.
18 O. Nováková, J. Malina, J. Kašpárková, A. Halámiková, V. Bernard, F. Intini, G. Natile and V. Brabec, *Chem. – A Eur. J.*, 2009, **15**, 6211–6221.
19 A. R. Kapdi and I. J. S. Fairlamb, *Chem. Soc. Rev.*, 2014, **43**, 4751–4777.
20 T. Lazarević, A. Rilak and Ž. D. Bugarčić, *Eur. J. Med. Chem.*, 2017, **142**, 8–31.
21 H. H. Repich, V. V. Orysyk, L. G. Palchykovska, S. I. Orysyk, Y. L. Zborovskii, O. V. Vasylchenko, O. V. Storozhuk, A. A. Biluk, V. V. Nikulina, L. V. Garmanchuk, V. I. Pekhnyo and M. V. Vovk, *J. Inorg. Biochem.*, 2017, **168**, 98–106.
22 S. Medici, M. Peana, V. M. Nurchi, J. I. Lachowicz, G. Crisponi and M. A. Zoroddu, *Coord. Chem. Rev.*, 2015, **284**, 329–350.

23 M. Fanelli, M. Formica, V. Fusi, L. Giorgi, M. Micheloni and P. Paoli, *Coord. Chem. Rev.*, 2016, **310**, 41–79.

24 Ž. D. Bugarčić, J. Bogojeski and R. van Eldik, *Coord. Chem. Rev.*, 2015, **292**, 91–106.

25 M. N. Alam and F. Huq, *Coord. Chem. Rev.*, 2016, **316**, 36–67.

26 B. Testa, *ChemMedChem*, 2007, **2**, 727–727.

27 M. J. Romero and P. J. Sadler, in *Bioorganometallic Chemistry Applications in Drug Discovery, Biocatalsis and Imaging*, eds. G. Jaouen and M. Salmain, Wiley CH-VCH Verlag GmbH, 2015, vol. Chapter 3, pp. 85–115.

28 F. Arnesano, A. Pannunzio, M. Coluccia and G. Natile, *Coord. Chem. Rev.*, 2015, **284**, 286–297.

29 S. A. Abramkin, U. Jungwirth, S. M. Valiahdi, C. Dworak, L. Habala, K. Meelich, W. Berger, M. A. Jakupec, C. G. Hartinger, A. A. Nazarov, M. Galanski and B. K. Keppler, *J. Med. Chem.*, 2010, **53**, 7356–7364.

30 D. Talancón, C. López, M. Font-Bardía, T. Calvet, J. Quirante, C. Calvis, R. Messeguer, R. Cortés, M. Cascante, L. Baldomà and J. Badia, *J. Inorg. Biochem.*, 2013, **118**, 1–12.

31 N. S. Ng, M. J. Wu, S. J. Myers and J. R. Aldrich-Wright, *J. Inorg. Biochem.*, 2018, **179**, 97–106.

32 Z. Zhang, C. Li, X. Sun, C. Gao, C. Yu, Q. Liu, L. Bai, Y. Qian, B. Yang, P. Dong and Y. Zhang, *Inorganica Chim. Acta*, 2017, **455**, 166–172.

33 J. Albert, R. Bosque, M. Crespo, J. Granell, C. López, R. Martín, A. González, A. Jayaraman, J. Quirante, C. Calvis, J. Badía, L. Baldomà, M. Font-Bardia, M. Cascante and R. Messeguer, *Dalt. Trans.*, 2015, **44**, 13602–13614.

34 F. Liu, S. Gou, F. Chen, L. Fang and J. Zhao, *J. Med. Chem.*, 2015, **58**, 6368–6377.

35 W. Villarreal, L. Colina-Vegas, C. Rodrigues De Oliveira, J. C. Tenorio, J. Ellena, F. C. Gozzo, M. R. Cominetti, A. G. Ferreira, M. A. B. Ferreira, M. Navarro and A. A. Batista, *Inorg. Chem.*, 2015, **54**, 11709–11720.

36 M. Frik, J. Fernández-Gallardo, O. Gonzalo, V. Mangas-Sanjuan, M. González-Alvarez, A. Serrano Del Valle, C. H. Hu, I. González-Alvarez, M. Bermejo, I. Marzo and M. Contel, *J. Med. Chem.*, 2015, **58**, 5825–5841.

37 A. Kumar, A. Naaz, A. P. Prakasham, M. K. Gangwar, R. J. Butcher, D. Panda and P. Ghosh, *ACS Omega*, 2017, **2**, 4632–4646.

38 X. Riera, V. Moreno, E. Freisinger and B. Lippert, *Inorganica Chim. Acta*, 2002, **339**, 253–264.

39 M. A. Peláez, T. Ramírez, M. Martínez, P. Sharma, C. Álvarez and R. Gutiérrez, *Zeitschrift fur Anorg. und Allg. Chemie*, 2004, **630**, 1489–1494.

40 M. Miller and E. Y. Tshuva, *Eur. J. Inorg. Chem.*, 2014, **9**, 1485–1491.

41 C. M. Manna, G. Armony and E. Y. Tshuva, *Chem. Eur. J.*, 2011, **17**, 14094–14103.

42 J. Vázquez, S. Berns, P. Sharma, J. Pérez, G. Hernández, A. Tovar, U. Peña and R. Gutiérrez, *Polyhedron*, 2011, **30**, 2514–2522.

43 S. Tabassum, A. Asim, R. A. Khan, F. Arjmand, D. Rajakumar, P. Balaji and M. A. Akbarsha, *RSC Adv.*, 2015, **5**, 47439–47450.

44 S. Newcombe, M. Bobin, A. Shrikhande, C. Gallop, Y. Pace, H. Yong, R. Gates, S. Chaudhuri, M. Roe, E. Hoffmann and E. M. E. Viseux, *Org. Biomol. Chem.*, 2013, **11**, 3255–3260.

45 X. Q. Zhou, Q. Sun, L. Jiang, S. T. Li, W. Gu, J. L. Tian, X. Liu and S. P. Yan, *Dalt. Trans.*, 2015, **44**, 9516–9527.

46 W. Ginzinger, G. Muehlgassner, V. B. Arion, M. A. Jakupec, A. Roller, M. Galanski, M. Reithofer, W. Berger and B. K. Keppler, *J. Med. Chem.*, 2012, **55**, 3398–3413.

47 M. S. I. El Alami, M. A. El Amrani, F. Agbossou-Niedercorn, I. Suisse and A. Mortreux, *Chem. - A Eur. J.*, 2015, **21**, 1398–1413.

48 R. M. Carman, P. C. Mathew, G. N. Saraswathi, B. Singaram and J. Verghese, *Aust. J. Chem.*, 1977, **30**, 1323–1335.

49 I. de la Cueva-Alique, S. Sierra, L. Muñoz-Moreno, A. Pérez-Redondo, A. M. Bajo, I. Marzo, L. Gude, T. Cuenca and E. Royo, *J. Inorg. Biochem.*, 2018, **183**, 32–42.

50 I. De La Cueva-Alique, L. Muñoz-Moreno, Y. Benabdelouahab, B. T. Elie, M. A. El Amrani, M. E. G. Mosquera, M. Contel, A. M. Bajo, T. Cuenca and E. Royo, *J. Inorg. Biochem.*, 2016, **156**, 22–34.

51 I. de la Cueva-Alique, S. Sierra, A. Perez-Redondo, I. Marzo, L. Gude, T. Cuenca and E. Royo, *J. Organomet. Chem.*, 2019, **881**, 150–158.

52 Y. Benabdelouahab, L. Muñoz-Moreno, M. Frik, I. de la Cueva-Alique, M. A. El Amrani, M. Contel, A. M. Bajo, T. Cuenca and E. Royo, *Eur. J. Inorg. Chem.*, 2015, **13**, 2295–2307.

53 V. Y. Kukushkin and A. J. L. Pombeiro, *Coord. Chem. Rev.*, 1999, **181**, 147–175.

54 M. A. Motaleb and A. A. Selim, *Bioorg. Chem.*, 2019, **82**, 145–155.

55 J. Reedijk, *Inorganica Chim. Acta*, 1992, **198**, 873–881.

56 E. Abele, R. Abele and E. Lukevics, *Chem. Heterocycl. Compd.*, 2009, **45**, 1420–1440.

57 E. Abele, R. Abele and E. Lukevics, *Chem. Heterocycl. Compd.*, 2008, **44**, 769–792.

58 E. Abele, R. Abele and E. Lukevics, *Chem. Heterocycl. Compd.*, 2008, **44**, 637–649.

59 C. Bartel, A. K. Bytzek, Y. Y. Scaffidi-Domianello, G. Grabmann, M. A. Jakupec, C. G. Hartinger, M. Galanski and B. K. Keppler, *J. Biol. Inorg. Chem.*, 2012, **17**, 465–474.

60 D. S. Bolotin, M. Y. Demakova, A. A. Legin, V. V. Suslonov, A. A. Nazarov, M. A. Jakupec, B. K. Keppler and V. Y. Kukushkin, *New J. Chem.*, 2017, **41**, 6840–6848.

61 N. Bandyopadhyay, P. Basu, G. S. Kumar, B. Guhathakurta, P. Singh and J. P. Naskar, *J. Photochem. Photobiol. B-Biology*, 2017, **173**, 560–570.

62 K. Karami, Z. M. Lighvan, A. M. Alizadeh, M. Poshteh-Shirani, T. Khayamian and J. Lipkowski, *RSC Adv.*, 2016, **6**, 78424–78435.

63 S. Wirth, C. J. Rohbogner, M. Cieslak, J. Kazmierczak-Baranska, S. Donevski, B. Nawrot and I. P. Lorenz, *J. Biol. Inorg. Chem.*, 2010, **15**, 429–440.

64 N. Chitrapriya, V. Mahalingam, M. Zeller, H. Lee and K. Natarajan, *J. Mol. Struct.*, 2010, **984**, 30–38.

65 N. Chitrapriya, V. Mahalingam, L. C. Channels, M. Zeller, F. R. Fronczek and K. Natarajan, *Inorganica Chim. Acta*, 2008,

361, 2841–2850.
66 Y. Fu, R. Soni, M. J. Romero, A. M. Pizarro, L. Salassa, G. J. Clarkson, J. M. Hearn, A. Habtemariam, M. Wills and P. J. Sadler, *Chem. - A Eur. J.*, 2013, **19**, 15199–15209.
67 E. T. J. Strong, S. A. Cardile, A. L. Brazeau, M. C. Jennings, R. Mcdonald and N. D. Jones, *Inorg. Chem.*, 2008, **47**, 10575–10586.
68 J.-Y. Lee, J.-Y. Lee, Y.-Y. Chang, C.-H. Hu, N. M. Wang and H. M. Lee, *Organometallics*, 2015, **34**, 4359–4368.
69 S. V Larionov, *Russ. J. Coord. Chem.*, 2012, **38**, 1–23; and references therein.
70 S. V. Larionov, T. E. Kokina, L. I. Myachina, L. A. Glinskaya, M. I. Rakhmanova, D. Y. Naumov, A. V. Tkachev and A. M. Agafontsev, *Russ. J. Coord. Chem.*, 2015, **41**, 162–168.
71 T. E. Kokina, L. A. Glinskaya, A. M. Agafontsev, E. V Artimonova, L. A. Sheludyakova, I. V Korol'kov, A. V Tkachev and S. V Larionov, *Russ. Chem. Bull.*, 2013, **62**, 2595–2602.
72 G. Chahboun, C. E. Petrisor, E. Gomez-Bengoa, E. Royo and T. Cuenca, *Eur. J. Inorg. Chem.*, 2009, **11**, 1514–1520.
73 M. Serratrice, L. Maiore, A. Zucca, S. Stoccoro, I. Landini, E. Mini, L. Massai, G. Ferraro, A. Merlino, L. Messori and M. A. Cinellu, *Dalt. Trans.*, 2016, **45**, 579–590.
74 B. T. Elie, J. Fernandez-Gallardo, N. Curado, M. A. Cornejo, J. W. Ramos and M. Contel, *Eur. J. Med. Chem.*, 2019, **161**, 310–322.
75 N. Lease, V. Vasilevski, M. Carreira, A. de Almeida, M. Sanau, P. Hirva, A. Casini, M. M. Contel, M. Sanaú, P. Hirva, A. Casini and M. M. Contel, *J. Med. Chem.*, 2013, **56**, 5806–5818.
76 P. Govender, T. Riedel, P. J. Dyson and G. S. Smith, *Dalt. Trans.*, 2016, **45**, 9529–9539.
77 V. Fernandez-Moreira, I. Marzo and M. Concepcion Gimeno, *Chem. Sci.*, 2014, **5**, 4434–4446.
78 L. Massai, J. Fernandez-Gallardo, A. Guerri, A. Arcangeli, S. Pillozzi, M. Contel and L. Messori, *Dalt. Trans.*, 2015, **44**, 11067–11076.
79 E. Guillen, A. Gonzalez, C. Lopez, P. K. Basu, A. Ghosh, M. Font-Bardia, C. Calvis and R. Messeguer, *Eur. J. Inorg. Chem.*, 2015, **22**, 3781–3790.
80 A. Mishra, S. C. Lee, N. Kaushik, T. R. Cook, E. H. Choi, N. K. Kaushik, P. J. Stang and K.-W. Chi, *Chem. Eur. J.*, 2014, **20**, 14410–14420.
81 J. Fernandez-Gallardo, B. T. Elie, F. J. Sulzmaier, M. Sanau, J. W. Ramos and M. Contel, *Organometallics*, 2014, **33**, 6669–6681.
82 D. Nieto, A. M. Gonzalez-Vadillo, S. Bruna, C. J. Pastor, C. Rios-Luci, L. G. Leon, J. M. Padron, C. Navarro-Ranninger and I. Cuadrado, *Dalt. Trans.*, 2012, **41**, 432–441.
83 M. L. Saha, X. Yan and P. J. Stang, *Acc. Chem. Res.*, 2016, **49**, 2527–2539.
84 Y. Zaidi, F. Arjmand, N. Zaidi, J. A. Usmani, H. Zubair, K. Akhtar, M. Hossain and G. G. H. A. Shadab, *Metallomics*, 2014, **6**, 1469–1479.
85 B. T. Elie, Y. Pechenyy, F. Uddin and M. Contel, *J. Biol. Inorg. Chem.*, 2018, **23**, 399–411.
86 J. L. Wedgwood, R. A. Kresinski, S. Merry and A. W. G. Platt, 2003, **95**, 149–156.
87 J. F. Gonzalez-Pantoja, M. Stern, A. A. A. Jarzecki, E. Royo, E. Robles-Escajeda, A. Varela-Ramirez, R. J. J. Aguilera and M. Contel, *Inorg. Chem.*, 2011, **50**, 11099–11110.
88 N. Bandyopadhyay, M. Zhu, L. Lu, D. Mitra, M. Das, P. Das, A. Samanta and J. P. Naskar, *Eur. J. Med. Chem.*, 2015, **89**, 59–66.
89 N. Bandyopadhyay, M. Das, A. Samanta, M. Zhu, L. Lu and J. P. Naskar, *Chemistryselect*, 2017, **2**, 230–240.
90 D. B. Dell'Amico, M. Colalillo, L. Dalla Via, M. Dell'Acqua, A. N. Garcia-Argaez, M. Hyeraci, L. Labella, F. Marchetti and S. Samaritani, *Eur. J. Inorg. Chem.*, 2018, 1589–1594.
91 M. Watanabe, Y. Kashiwame, S. Kuwata and T. Ikariya, *Eur. J. Inorg. Chem.*, 2012, **3**, 504–511.
92 A. Erxleben, J. Claffey and M. Tacke, *J. Inorg. Biochem.*, 2010, **104**, 390–396.
93 J. H. Toney and T. J. Marks, *J. Am. Chem. Soc.*, 1985, **107**, 947–953.
94 T. S. Morais, F. C. Santos, T. F. Jorge, L. Côrte-Real, P. J. A. Madeira, F. Marques, M. P. Robalo, A. Matos, I. Santos and M. H. Garcia, *J. Inorg. Biochem.*, 2014, **130**, 1–14.
95 F. Aman, M. Hanif, W. A. Siddiqui, A. Ashraf, L. K. Filak, J. Reynisson, T. Söhnel, S. M. F. Jamieson and C. G. Hartinger, *Organometallics*, 2014, **33**, 5546–5553.
96 H. P. Varbanov, S. Göschl, P. Heffeter, S. Theiner, A. Roller, F. Jensen, M. A. Jakupec, W. Berger, M. Galanski and B. K. Keppler, *J. Med. Chem.*, 2014, **57**, 6751–6764.
97 A. R. Ghezzi, M. Aceto, C. Cassino, E. Gabano and D. Osella, *J. Inorg. Biochem.*, 2004, **98**, 73–78.
98 J. A. Platts, S. P. Oldfield, M. M. Reif, A. Palmucci, E. Gabano and D. Osella, *J. Inorg. Biochem.*, 2006, **100**, 1199–1207.
99 I. V. Tetko, I. Jaroszewicz, J. A. Platts and J. Kuduk-Jaworska, *J. Inorg. Biochem.*, 2008, **102**, 1424–1437.
100 K. Takács-Novák, A. Avdeef, K. J. Box, B. Podányi and G. Szász, *J. Pharm. Biomed. Anal.*, 1994, **12**, 1369–1377.
101 C. Cullinane, G. B. Deacon, P. R. Drago, A. P. Erven, P. C. Junk, J. Luu, G. Meyer, S. Schmitz, I. Ott, J. Schur, L. K. Webster and A. Klein, *Dalt. Trans.*, 2018, **47**, 1918–1932.
102 N. P. Farrell, *Chem. Soc. Rev.*, 2015, **44**, 8773–8785.
103 J. B. Chaires, in *DNA Binders and Related Subjects*, eds. M. J. Waring and J. B. Chaires, Springer-Verlag Berlin, Berlin, 2005, vol. 253, pp. 33–53.
104 D. Renciuk, J. Zhou, L. Beaurepaire, A. Guedin, A. Bourdoncle and J. L. Mergny, *Methods*, 2012, **57**, 122–128.
105 R. Kieltyka, P. Englebienne, J. Fakhoury, C. Autexier, N. Moitessier and H. F. Sleiman, *J. Am. Chem. Soc.*, 2008, **130**, 10040–10041.
106 D. Suh and J. B. Chaires, *Bioorg. Med. Chem.*, 1995, **3**, 723–728.
107 G. Cohen and H. Eisenberg, *Biopolymers*, 1969, **8**, 45–55.
108 T. A. Fairley, R. R. Tidwell, I. Donkor, N. A. Naiman, K. A. Ohemeng, R. J. Lombardy, J. A. Bentley and M. Cory, *J. Med. Chem.*, 1993, **36**, 1746—1753.
109 N. Sohrabi, N. Rasouli and M. Kamkar, *Bull. Korean Chem. Soc.*, 2014, **35**, 2523–2528.
110 G. Yang, J. Z. Wu, L. Wang, L. N. Ji and X. Tian, *J. Inorg.*

Biochem., 1997, **66**, 141–144.
111 L.-F. Tan and H. Chao, *Inorganica Chim. Acta*, 2007, **360**, 2016–2022.
112 G. Y. Park, J. J. Wilson, Y. Song and S. J. Lippard, *Proc. Natl. Acad. Sci. U. S. A.*, 2012, **109**, 11987–11992.
113 K. S. Lovejoy, R. C. Todd, S. Zhang, M. S. McCormick, J. A. D'Aquino, J. T. Reardon, A. Sancar, K. M. Giacomini and S. J. Lippard, *Proc. Natl. Acad. Sci. U. S. A.*, 2008, **105**, 8902–8907.
114 T. Peleg-Shulman, J. Katzhendler and D. Gibson, *J. Inorg. Biochem.*, 2000, **81**, 313–323.
115 S. Cruz, S. Bernès, P. Sharma, R. Vazquez, G. Hernández, R. Portillo and R. Gutiérrez, *Appl. Organomet. Chem.*, 2010, **24**, 8–11.
116 A. S. Abu-Surrah, M. Kettunen, M. Leskelä and Y. Al-Abed, *Zeitschrift fur Anorg. und Allg. Chemie*, 2008, **634**, 2655–2658.
117 T. V. Segapelo, S. Lillywhite, E. Nordlander, M. Haukka and J. Darkwa, *Polyhedron*, 2012, **36**, 97–103.
118 D. Gutiérrez, S. Bernès, G. Hernández, O. Portillo, G. E. Moreno, M. Sharma, P. Sharma and R. Gutiérrez, *J. Coord. Chem.*, 2015, **68**, 3805–3813.
119 D. Ning, Y. Cao, Y. Zhang, L. Xia and G. Zhao, *Inorg. Chem. Commun.*, 2015, **58**, 57–59.
120 A. A. Shabana, I. S. Butler, A. Castonguay, M. Mostafa, B. J. Jean-Claude and S. I. Mostafa, *Polyhedron*, 2018, **154**, 156–172.
121 T. T. H. Fong, C. N. Lok, C. Y. S. Chung, Y. M. E. Fung, P. K. Chow, P. K. Wan and C. M. Che, *Angew. Chemie - Int. Ed.*, 2016, **55**, 11935–11939.
122 D. Kovala-Demertzi, A. Boccarelli, M. A. Demertzis and M. Coluccia, *Chemotherapy*, 2007, **53**, 148–152.
123 O. Kacar, Z. Adiguzel, V. T. Yilmaz, Y. Cetin, B. Cevatemre, N. Arda, A. T. Baykal, E. Ulukaya and C. Acilan, *Anticancer. Drugs*, 2014, **25**, 17–29.
124 E. Ulukaya, F. Ari, K. Dimas, M. Sarimahmut, E. Guney, N. Sakellaridis and V. T. Yilmaz, *J. Cancer Res. Clin. Oncol.*, 2011, **137**, 1425–1434.
125 M. Mareel and A. Leroy, *Physiol. Rev.*, 2003, **83**, 337–376.
126 W. G. Jiang, A. J. Sanders, M. Katoh, H. Ungefroren, F. Gieseler, M. Prince, S. K. Thompson, M. Zollo, D. Spano, P. Dhawan, D. Sliva, P. R. Subbarayan, M. Sarkar, K. Honoki, H. Fujii, A. G. Georgakilas, A. Amedei, E. Niccolai, A. Amin, S. S. Ashraf, L. Ye, W. G. Helferich, X. Yang, C. S. Boosani, G. Guha, M. R. Ciriolo, K. Aquilano, S. Chen, A. S. Azmi, W. N. Keith, A. Bilsland, D. Bhakta, D. Halicka, S. Nowsheen, F. Pantano and D. Santini, *Semin. Cancer Biol.*, 2015, **35**, S244–S275.
127 J. Cao, Q. Wu, W. Zheng, L. Li and W. Mei, *RSC Adv.*, 2017, **7**, 26625–26632.
128 C. Mu, S. W. Chang, K. E. Prosser, A. W. Y. Leung, S. Santacruz, T. Jang, J. R. Thompson, D. T. T. Yapp, J. J. Warren, M. B. Bally, T. V Beischlag and C. J. Walsby, *Inorg. Chem.*, 2016, **55**, 177–190.
129 M. N. Zivanovic, J. V Kosaric, B. Smit, D. S. Seklic, R. Z. Pavlovic and S. D. Markovic, *Gen. Physiol. Biophys.*, 2017, **36**, 187–196.
130 E. Ulukaya, F. Ari, K. Dimas, E. I. Ikitimur, E. Guney and V. T. Yilmaz, *Eur. J. Med. Chem.*, 2011, **46**, 4957–4963.
131 M. S. Ibn El Alami, M. A. El Amrani, A. Dahdouh, P. Roussel, I. Suisse and A. Mortreux, *Chirality*, 2012, **24**, 675–682.
132 D. Brecknell, R. Carman, B. Singaram and J. Verghese, *Aust. J. Chem.*, 1977, **30**, 195.
133 G. E. Tranter, *8.21 Spectroscopic Analysis: Polarimetry and Optical Rotatory Dispersion*, Elsevier Ltd., 2012, vol. 8.